

UNIVERSIDADE ESTADUAL DE CAMPINAS
SISTEMA DE BIBLIOTECAS DA UNICAMP
REPOSITÓRIO DA PRODUÇÃO CIENTÍFICA E INTELECTUAL DA UNICAMP

Versão do arquivo anexado / Version of attached file:

Versão do Editor / Published Version

Mais informações no site da editora / Further information on publisher's website:

<https://www.frontiersin.org/journals/immunology/articles?publication-date=01%2F06%2F2021-01%2F07%2F2021&type=99§ion=559>

DOI: 10.3389/fimmu.2021.689519

Direitos autorais / Publisher's copyright statement:

©2021 by Frontiers Research Foundation. All rights reserved.

DIRETORIA DE TRATAMENTO DA INFORMAÇÃO

Cidade Universitária Zeferino Vaz Barão Geraldo

CEP 13083-970 – Campinas SP

Fone: (19) 3521-6493

<http://www.repositorio.unicamp.br>



Recent Advances in Immunosafety and Nanoinformatics of Two-Dimensional Materials Applied to Nano-imaging

Gabriela H. Da Silva¹, Lidiane S. Franqui^{1,2}, Romana Petry^{1,3}, Marcella T. Maia¹, Leandro C. Fonseca⁴, Adalberto Fazzio^{1,3}, Oswaldo L. Alves^{4*} and Diego Stéfani T. Martinez^{1,2*}

¹ Brazilian Nanotechnology National Laboratory (LNNano), Brazilian Center for Research in Energy and Materials (CNPEM), Campinas, Brazil, ² School of Technology, University of Campinas (Unicamp), Limeira, Brazil, ³ Center of Natural and Human Sciences, Federal University of ABC (UFABC), Santo Andre, Brazil, ⁴ NanoBioss Laboratory and Solid State Chemistry Laboratory (LQES), Institute of Chemistry, University of Campinas (Unicamp), Campinas, Brazil

OPEN ACCESS

Edited by:

Diana Boraschi,
Shenzhen Institutes of Advanced
Technology, Chinese Academy of
Sciences (CAS), China

Reviewed by:

Paola Italiani,
National Research Council (CNR), Italy
Mariusz Piotr Madej,
Oceano B.V., Netherlands

*Correspondence:

Oswaldo L. Alves
izolas@unicamp.br
Diego Stéfani T. Martinez
diego.martinez@lnnano.cnpe.br

Specialty section:

This article was submitted to
Molecular Innate Immunity,
a section of the journal
Frontiers in Immunology

Received: 01 April 2021

Accepted: 10 May 2021

Published: 03 June 2021

Citation:

Da Silva GH, Franqui LS, Petry R,
Maia MT, Fonseca LC, Fazzio A,
Alves OL and Martinez DST (2021)
Recent Advances in Immunosafety
and Nanoinformatics of
Two-Dimensional Materials
Applied to Nano-imaging.
Front. Immunol. 12:689519.
doi: 10.3389/fimmu.2021.689519

Two-dimensional (2D) materials have emerged as an important class of nanomaterials for technological innovation due to their remarkable physicochemical properties, including sheet-like morphology and minimal thickness, high surface area, tuneable chemical composition, and surface functionalization. These materials are being proposed for new applications in energy, health, and the environment; these are all strategic society sectors toward sustainable development. Specifically, 2D materials for nano-imaging have shown exciting opportunities in *in vitro* and *in vivo* models, providing novel molecular imaging techniques such as computed tomography, magnetic resonance imaging, fluorescence and luminescence optical imaging and others. Therefore, given the growing interest in 2D materials, it is mandatory to evaluate their impact on the immune system in a broader sense, because it is responsible for detecting and eliminating foreign agents in living organisms. This mini-review presents an overview on the frontier of research involving 2D materials applications, nano-imaging and their immunosafety aspects. Finally, we highlight the importance of nanoinformatics approaches and computational modeling for a deeper understanding of the links between nanomaterial physicochemical properties and biological responses (immunotoxicity/biocompatibility) towards enabling immunosafety-by-design 2D materials.

Keywords: nanomaterials, bioimaging, immunotoxicity, nanobiotechnology, nanosafety

INTRODUCTION

Two-dimensional (2D) materials constitutes an emerging class of nanomaterials, characterized mainly by their high surface-area-to-mass ratio due to a sheet-like morphology; responsible for their outstanding physicochemical properties (e.g., electronic, optical, mechanical, and magnetic) with a currently leading position in materials science and technology (1, 2). Since the pioneering work of

Novoselov et al. (3) in 2004, several 2D materials have been produced for many applications in energy, catalysis, composites, sensors, biomedicine, agriculture, and environmental remediation (4–7).

Beyond graphene-based materials (GBMs), other 2D materials have also emerged, by replacing carbon elements for other heteroatoms (P, B, O, and N) (8). Black phosphorus (BP), transition metal dichalcogenides (TMDs), transition metal carbides, nitrides, and carbonitrides (MXenes), layered double hydroxides (LDHs), antimonenes (AM), boron nitride nanosheets (BNNs) are the most common graphene analogs under investigation (9–17).

Among several applications, 2D materials have attracted special interest to be applied in the bioimaging field because of their high electrical and thermal conductivity, high degree of anisotropy, exceptional mechanical strength, and unique optical properties (18). Due to such properties, 2D materials have been developed to be applied in molecular imaging techniques, such as computed tomography (CT), magnetic resonance imaging (MRI), optical imaging (fluorescence and luminescence), and nuclear imaging including positron emission tomography (PET) and single photon emission computed tomography (SPECT) (19). Besides, 2D materials allow multimodal imaging by providing a variety of properties useful for more than one imaging technique and/or because of their facility to combine them to form nanocomposites and hybrid materials (20). Given the applicability and growing interests in 2D materials, unveiling their impact on the immune system is a key step towards safe use and responsible innovation (21, 22). These materials' intrinsic characteristics, such as chemical composition, surface chemistry, functionalization, morphology, lateral size, purity, and crystallinity are directed related to their degradability, dispersion stability, and protein corona profile; hence, their adverse effects in a biological system (23–26). Such parameters modulate the biotransformation and biodistribution of 2D materials under *in vitro* and *in vivo* models, influencing their interaction with the immune system, fate, and toxicological profile (27–30).

Biocompatibility, biodegradability, and eliciting an adequate biological effect in the organisms are crucial to the applicability of 2D materials (22, 24, 31). Indeed, the complexity of toxicokinetic and toxicodynamic events of 2D materials under physiological conditions associated with a lack of harmonized protocols for experimental research represents majors challenges for clinical translation and safety regulation involving these emerging materials (32–35). Therefore, combining systems toxicology and nanoinformatics is a foremost strategy in the integration of 2D material design on a safe and sustainable basis (36–38).

In this mini-review, we present the recent advances involving 2D materials, nano-imaging, and immunosafety. Briefly, the main findings associated with the adverse immunological effects were shown in *in vitro* and *in vivo* models. Finally, we highlight the great potential of nanoinformatics approaches towards immunosafety-by-design 2D materials (Figure 1).

TECHNOLOGICAL APPLICATIONS AND INNOVATION OF 2D MATERIALS

A literature review on the Web of ScienceTM database was performed, considering articles published from 2000 to 2021 (25/03/2021), and over these last 20 years, many 2D materials have been synthesized as exemplified in Figure 2A. The number of publications of 2D materials and their applications is growing, in which nano-imaging and drug release systems stand out and are present mostly in the health sector (Figures 2B, D). For energy application, the structural and electronic properties of 2D materials have been shown to improve the energy accumulation in devices such as lithium-ion, metal-air batteries (LIBs) (9, 39, 49, 50) and electrochemical devices (51, 52). Moreover, these 2D materials are of particular interest as catalysts and nanoscale substrates, replacing transition, or noble metals normally used to catalyze an acid-basic reaction, producing metal free-catalysts (53, 54). In environment, the 2D materials have been used as adsorbents for removing pollutants to treat contaminated water (55–57). Their atomic thickness and antibacterial activity contribute to superior water permeability and anti-fouling capacity in the development of membranes for desalination (58–62) and cleaning purposes (63–65). Sensing has covered both environmental and health sectors, contributing to the detection and monitoring of traces of pollutants (66, 67) and blood biomarkers (68–71). The thin structure, large surface area, chemical modifications and quenching ability of 2D materials provide high sensitivity, durability, stability, selectivity, and conductivity for sensors and biosensors (72–82).

Considering biomedical applications, 2D materials have been applied in bone tissue engineering, conferring improved mechanical characteristics and great osteoconductivity for scaffold design (83–87). However, due to the higher surface area of 2D materials and distinguish light-material interactions, research has mostly given attention to their usefulness in nano-imaging and therapeutics (theranostics) (88) (Figures 2B, C), including early detection, monitoring, and treatment of diseases, which are the main examples described in this mini-review (89). For example, in cancer, malign tumors are sensitive to heating when compared to healthy tissues. Graphene oxide decorated with gold nanoparticles (GO-AuNPs), TMDs (MoS₂, WS₂), and MXenes (MoC₂, Ti₃C₂) have shown effective agents in photothermal and photodynamic therapy for inducing tumor necrosis (40, 41, 90–92). 2D materials have been successfully modified with numerous polymers to enhance their cytocompatibility and dispersibility (90) and used as nanoplateforms carrying active molecules or imaging agents to improve their biological function (93) and clinical visualization for imaging-drug delivery guiding (12, 94). MoS₂ and BNNs have been employed as effective fluorescence quenchers and associated with aptamers, substituting antibody-based therapy (69, 95–97). Compared to the other 2D inorganic materials, and in addition to the previous features, the ultrathin structure of the BP nanosheets results in an exceptional biodegradability in physiological media it shows promising in theranostics (98, 99). Magnetic nanoparticles have been used as contrast agents

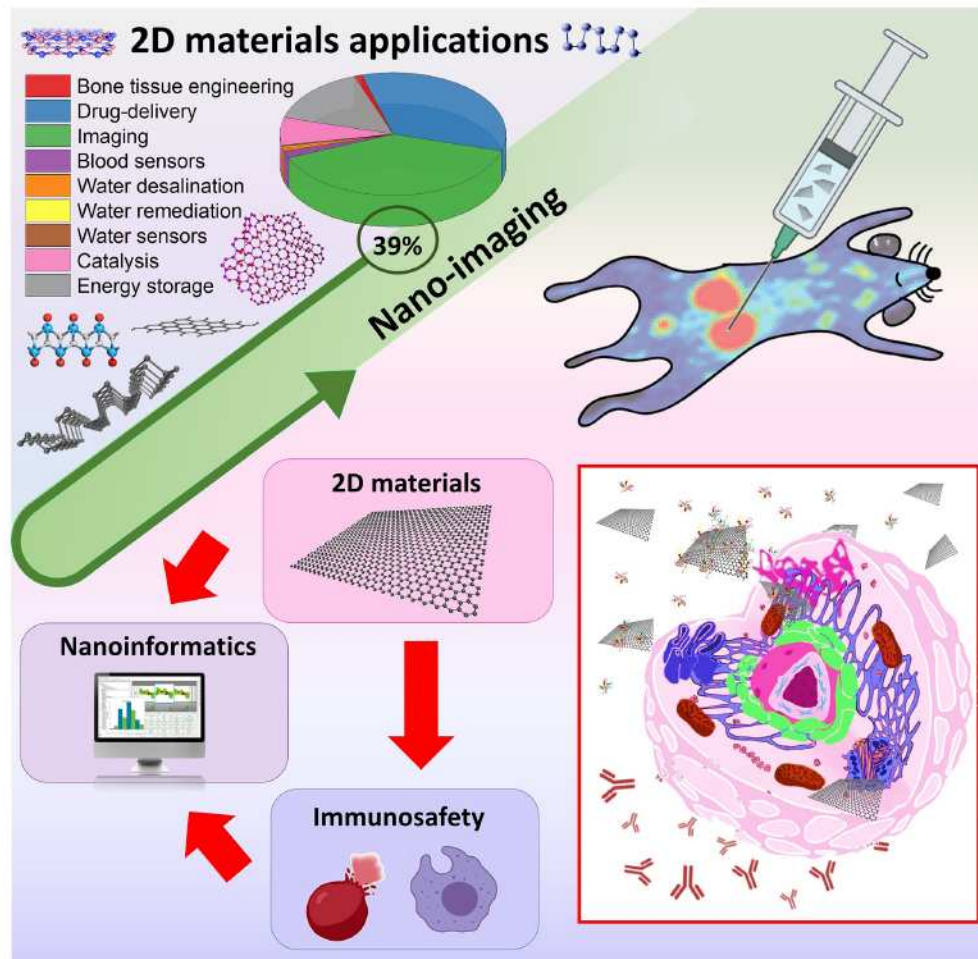


FIGURE 1 | Two-dimensional materials applications, nano-imaging and their links with immunosafety and nanoinformatics approaches.

and incorporated into 2D materials in MRI, in place of conventional ones (100, 101). In this respect, 2D magnetic materials production can be very useful for accurate bioimaging and therapy of diseases *in vivo* using MRI and CT techniques (10, 102).

2D MATERIALS AND THE IMMUNE SYSTEM: ADVERSE EFFECTS IN *IN VITRO* AND *IN VIVO* MODELS

As far as it is known, 2D materials have proven their significance and innovation perspective in almost all industrial areas and sectors, making it imperative to assess their environmental health risks and safety aspects (24, 103–105). However, toxicological studies, including immunotoxicity, are still in their infancy for GBMs and 2D inorganic materials (31). Table 1 is an extensive literature revision reporting major findings of 2D materials and their adverse effects in the

immunological system considering *in vitro* and *in vivo* models. The terms used for the literature research is detailed in the supplementary material.

Studies have demonstrated that 2D materials can induce immunological system activation with a consequent induction of an inflammatory response (145). This immunological system activation showed itself to be dependent of the 2D materials' physicochemical properties, such as size (106–109, 144), surface chemistry (114, 115, 123), number of layers, shape (118, 119), and functionalization (109, 112, 114, 128, 135, 139). For example, Yue et al. (106) demonstrated that larger graphene oxide (GO) (2 μm) has induced a higher immunological activation than smaller GO (350 nm) both *in vitro* (peritoneal macrophages) and *in vivo* (C57BL/6 mice). Similarly, Ma et al. (107) showed a lateral-size-dependent pro-inflammatory effect of GO under *in vitro* and *in vivo* conditions, wherein the largest GO (L-GO; 750–1300 nm) elicit higher inflammatory response than smallest GO (S-GO; 50–350 nm). Moreover, the mechanism of inflammation has also differed according to the lateral size, with L-GO being more prone to plasma membrane adsorption and the toll-like receptors

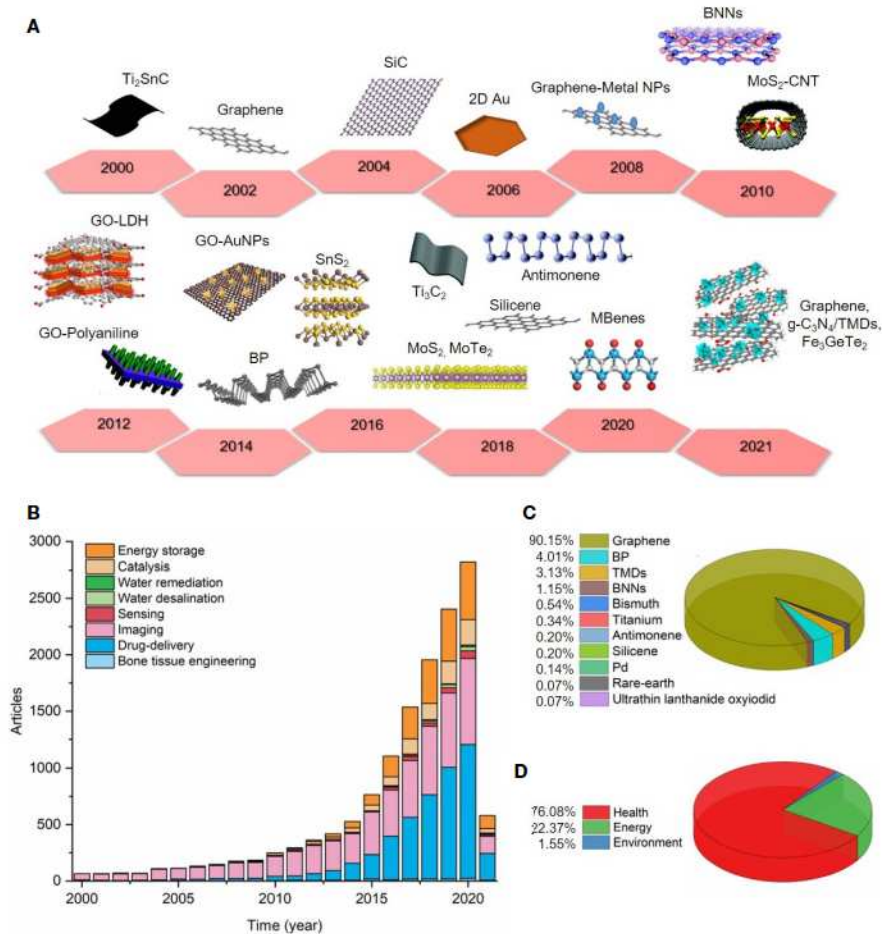


FIGURE 2 | The data obtained previously was organized into the following sectors: health (bone tissue engineering, drug delivery, imaging, sensing blood markers), energy (catalysis and energy storage), and environment (water remediation and desalination, and water sensing contaminants). **(A)** Timeline showing examples of 2D materials produced over the period established (from 2000 to 2021). **(B)** Number of articles from 2000 to 2021 (25/03/2021). **(C)** 2D materials used in nano-imaging applications (see supporting information). **(D)** Percentage of 2D materials applied in health, energy and environment sectors.

(TLRs) and nuclear factor- κB (NF- κB) pathways activation, whereas S-GO was mostly taken up by macrophages. In another study that investigated the effects of small GO (S-GO < 1 μm) and large GO (L-GO, 1–10 μm) on human peripheral immune cells, it was found that the S-GO has a more significant impact on the upregulation of critical genes implicated in immune responses and the release of cytokines IL1 β and TNF α compared to L-GO (108). However, it is important to clarify here that the S-GO in this study presented similar lateral size of the L-GO in the previous studies cited, which means that all these studies are in agreement, and we may erroneously interpret them because attention to the lateral size was not devoted. Indeed, a nomenclature harmonization of GBMs is urgently needed to allow a clear understanding on the impacts of GBM physicochemical properties on their biocompatibility.

Besides to assess the effect of lateral size, Duarte and coworkers (109) investigated the impacts of two different surfaces functionalization: pegylated graphene oxide (GO-PEG,

200–500 nm) and flavin mononucleotide-stabilized pristine graphene with two different sizes (200–400 nm and 100–200 nm). Their results showed that the cellular uptake of GBMs was mainly influenced by their lateral size, with smaller particles showing greater internalization, while the inflammatory response depended also on the type of functionalization, with GO-PEG showing the lower pro-inflammatory potential. This study corroborates in number previous ones that also showed an increased biocompatibility of GO due to the pegylation (GO-PEG) (110, 111). Similarly, Xie et al. (139) studied PEG coated 2D titanium nanosheets (TiNS-PEG) and reported no indication of inflammation and other negative impacts. Moreover, the material was promising for photothermal tumor therapy and presented a high contrast for *in vivo* imaging. However, Gu et al. (129) found that MoS_2 and PEGylated MoS_2 induced a robust macrophage immune response, with PEG- MoS_2 eliciting stronger cytokine secretion than the pristine MoS_2 . By performing molecular dynamics simulations, they

TABLE 1 | Relevant studies addressing the adverse immunological effects of 2D materials in *in vitro* and *in vivo* models from 2000 to 2021.

Nanomaterial	Dose	Exposure time	<i>in vivo/in vitro</i> models	Method or endpoints	Adverse immunological effects	Ref.
Graphene oxide (GO) (lateral size of 350 nm and 2 μ m)	2, 4, and 6 μ g ml ⁻¹	24, 48, and 96 h	peritoneal macrophage	Secretion of pro-inflammatory cytokines (IL-6, IL-10, IL-12, TNF- α , MCP-1, and IFN- γ)	Dose-dependent release of cytokines induced in a higher extent by 2 μ m GO than 350 nm GO.	(106)
	–	21 days	C57BL/6 male mice	Histological micrographics	Mononuclear cells (i.e. macrophages and lymphocytes) infiltration and inflammation response induced by 2 μ m GO, but not by 350 nm GO.	
GO (smallest S-GO 50–350 nm; intermediate I-GO 350–750 nm; largest L-GO 750–1300 nm)	Viability: 1–300 μ g ml ⁻¹ ; Others: 20 μ g ml ⁻¹	12, 24 h	J774.A1 and THP-1 macrophages	Live/dead assay, TNF- α , IL-6 and IL1 β release; and macrophage polarization, NF- κ B signaling activation.	All GO materials have induced a decrease in cell viability, and a production of cytokines. The L-GO significantly elicited higher response than S-GO. Higher macrophage polarization to the M1 phenotype by L-GO than S-GO.	(107)
	<i>Ip</i> ¹ : 5000 μ g kg ⁻¹ bw; Lung ² : 2500 μ g kg ⁻¹ bw; It ³ : 5000 μ g kg ⁻¹ bw	<i>Ip</i> : 72 h; Lung: 72 h; It: 24 h	BALB/c male mice	Local and systemic inflammation: TNF- α , IL6 release, recruitment of immune cell.	Both S-GO and L-GO have induced an inflammatory response by cytokines production and leukocytes recruitment, been the L-GO response higher than the S-GO response in all endpoints.	
GO S-GO (<1 μ m) L-GO (1–10 μ m)	25, 50, and 75 μ g ml ⁻¹	24 h	PBMCs, Jurkat and THP-1 cells	Annexin-V FITC (apoptosis), LIVE/DEAD FITC (late apoptosis and necrosis), and propidium iodide (necrosis), cell activation (expression of CD69 and CD25 markers), cytokine release, expression of 84 genes related to innate and adaptive immune responses	Only S-GO presented a decrease in cell viability at highest dose (75 μ g/ml). None of GO tested have induced the cell activation (expression of CD69 and CD25 markers). However, both GO induced cytokines release and upregulation of genes related to immune response, being that the S-GO response was significantly higher compared to L-GO response.	(108)
GO-PEG (200–500 nm) and PG-FMN (L) (200–400 nm) and PG-FMN (S) (100–200 nm)	10 μ g ml ⁻¹	24 h	RAW-264.7 macrophages	Cellular uptake, nitric oxide production, NMR metabolic profiling, expression of cell surface markers CD80 and CD206.	PG-FMN (S) was internalized in a greater extent compared to GO-PEG and PG-FMN (L), which presented a similar uptake. GO-PEG did not induce NO production, whereas PG-FMN (S) and PG-FMN (L) caused significant NO increases of 21% and 12%, respectively. Only PG-FMN (S) caused increases in intracellular succinate and itaconate, similarly to LPS, while PG-FMN (L) did not alter the levels of TCA cycle intermediates and GO-PEG caused a decrease of succinate. Besides, GO-PEG decreased the TNF- α secretion compared to control cell, and do not affected the cell surface markers.	(109)
GO-PEG (200–500 nm)	40 and 80 μ g ml ⁻¹	24 and 48 h	Murine peritoneal macrophages	Cell surface markers of M1 (CD80 and iNOS) and M2 (CD206 and CD163) phenotypes.	PEG-GO did not induce the macrophage polarization towards the M1 pro-inflammatory phenotype, with a slight shift towards M2 reparative phenotype.	(110)
GO-1PEG (~100 nm) GO-6PEG (~300 nm)	2.3–75 μ g ml ⁻¹	24 h	RAW-264.7 macrophages and primary splenocytes (B-cells and T-cells)	Proinflammatory cytokine secretion (IL-1 β , TNF- α and IL-6) and proliferation of immune cells.	Only GO-6PEG increased the secretion of TNF- α by RAW-264.7 macrophages without alteration of IL-6 and IL-1 β levels. The treatment of primary splenocytes with GO-1PEG and GO-6PEG in the presence of concanavalin A, anti-CD3 antibody, and LPS, produced significant dose-dependent decrease of cell proliferation and IL-6 levels.	(111)
GO and PVP coated-GO	25, 50, and 100 μ g ml ⁻¹	48 h	Human DC, macrophages and T cells	Differentiation and maturation of DC cells, cytokine release, apoptosis of T cells, and phagocytosis	GO induced the differentiation and maturation of DC cells; a dose-dependent release of pro-inflammatory cytokines by DC cells; a dose-dependent apoptosis of T cells; and a susceptibility of phagocytosis by macrophages. The coating with PVP has reduced the cytokines secretion and the differentiation and maturation of DC cells; delayed the apoptotic process of T cells; and avoid the phagocytosis by macrophages.	(112)

(Continued)

TABLE 1 | Continued

Nanomaterial	Dose	Exposure time	<i>in vivo/in vitro</i> models	Method or endpoints	Adverse immunological effects	Ref.
GO GO-NH ₂ , GO-PAM, GO-PAA GO-PEG	1, 2, 4, 10, 20, 50, 100, or 200 µg ml ⁻¹	1, 6, and 24 h	J774A.1 cell line	Viability, cellular adhesion, uptake, membrane permeability and fluidity, Ca ²⁺ flux and transcriptome analysis.	GO caused the impairment of cell membrane integrity and functions including regulation of membrane- and cytoskeleton- associated genes, membrane permeability, fluidity, and ion channels. The -NH ₂ and -PAA showed similar toxicity to GO, but -PEG and -PAA significantly decreased the GO cytotoxicity.	(113)
	It: 1 mg kg ⁻¹	24 h	Male BALB/c mice	Survival, body weight increase, complete blood count (numbers of RBC, WBC, PLT, neutrophils, lymphocyte), blood biochemistry, GO distribution, histological analysis of lung, liver and spleen.	GO induced platelet depletion, pro-inflammatory response and pathological changes of lung and liver in mice. The -NH ₂ , -PAA and -PEG modifications greatly reduced the toxicity of GO in mice. The -PAM modification was more toxic than pristine GO.	
GO and reduced GO (rGO) (100 nm)	20, 40, 60, 80, and 100 µg ml ⁻¹	24 h	THP-1 cells	Cellular viability, proliferation, oxidative stress, mitochondrial membrane potential, ATP synthesis, antioxidants, apoptosis, DNA damage, and the inflammation response	Both GO and rGO caused dose-dependent loss of cell viability and proliferation, increased level of LDH, MMP, decreased level of ATP content, redox imbalance, mitochondria-mediated apoptosis, cell death due to oxidative stress, increased secretion of various cytokines and chemokines. Overall, the toxic response of rGO was more severe than GO for all endpoints.	(114)
GO nanoplatelets (GONPs) and reduced GONPs (rGONPs)	GONP (5 µg ml ⁻¹) or rGONP (50 µg ml ⁻¹)	24 h	THP-1 cells	Cell viability, ROS production, expression of genes related to the oxidative and inflammatory response, cellular uptake, endocytosis and phagocytosis, Rho/ROCK pathway, cytoskeleton analysis, differentiation of THP-1 cells into macrophage-like cells (THP-1a)	Both GO induced a dose-dependent loss in cell viability, an increase in ROS production, and a disruption of the F-actin cytoskeletons leading to the loss of the adherence ability of THP-1a and a reduction in the phagocytosis capability of THP-1a cells. GONP presented higher upregulation of HO-1 and SOD-2 expressions, and higher levels of IL-1β, TNF-α, IL-8, and MCP-1, compared to rGONP. rGONP exhibited a greater expression of NF-κB (p65), higher uptake and a higher decrease of Rho/ROCK expression than GONP.	(115)
Pristine graphene with 1% pluronic F108	20 µg ml ⁻¹	24 h	Primary and immortalized (RAW264.7) macrophages	Quantification of cytokines and chemokines (IFN-γ, IL-1α, IL-2, IL-4, IL-5, IL-6, IL-10, IL-17, TNFα, and GM-CSF, MCP-1, MCP-3, RANTES, MIP-1α and MIP-1β). RT-PCR analysis of the mRNA levels of TNF-α, IL-1β, IL-6, iNOS and COX-2. Adhesion, phagocytosis and cytoskeleton assay.	Increased transcription and secretion of cytokines and chemokines, which is triggered by activation of the NF-κB signaling pathway; The cytokines and chemokines secreted by graphene-exposed macrophages further impaired the morphology of naïve macrophages by affect the actin structures and podosomes expansion, decreasing the adhesion and phagocytosis.	(116)
Pristine graphene with 1% pluronic F108 (500–1000 nm)	20 µg ml ⁻¹	12, 24, and 48 h	Murine RAW 264.7 macrophages	Cell viability, ROS production, MMP, apoptosis, expression of proteins (Phospho-p38 MAPKinase (P-p38), p38 MAPKinase (p38), Phospho-JNK (P-JNK), JNK, Phospho-ERK (P-ERK), ERK, Phospho- Smad2, Smad2, Bim, Bax, caspase 3, Bcl-2, PARP and β-actin) and genes (TNF-α, TGF-β TGF-β receptor I, TGF-β receptor II, Smad2, Smad3, Smad4, Smad7, β-Actin)	Loss of cell viability at highest concentration (100 µg/ml); induction of intracellular ROS generation, depletion of MMP and apoptosis, all in a time- and dose-dependent way; activation of the mitochondrial pathways: MAPKs (JNK, ERK and p38) as well as the TGF-β-related signaling pathways.	(117)
Graphene nanoplatelets (1–10 layers)	1, 5 and 10 µg cm ²	24 h	THP-1 macrophages	Phagocytosis, cytokine release and the involvement of the NALP3 inflammasome.	Frustrated phagocytosis, loss of membrane integrity at higher concentration, increase in cytokines expression, and activation of the NALP3 inflammasome.	(118)
	pharyngeal aspiration: 50 µg per mouse.	24 h	C57BL/6 strain mice	BAL cells analysis, Histological sections of lungs. Pleural space lavage: total and differential cell	BAL and pleural lavage showed an increased number of polymorphonuclear leucocytes (neutrophils and eosinophils); and an increase in the levels of cytokines.	

(Continued)

TABLE 1 | Continued

Nanomaterial	Dose	Exposure time	<i>in vivo/in vitro</i> models	Method or endpoints	Adverse immunological effects	Ref.
	intrapleural injection: 5 μg per mouse			count, histological examination of the parietal pleura.	Histological analysis: presence of granulomatous lesions in the bronchiole lumen and near the alveolar region; presence of histiocytic aggregates along the mesothelium.	
Graphene nanoplatelets (~10 layers; particle size ~2 μm ; thickness ~3–4 nm)	Intratracheal instillation: 1.25, 2.5 and 5 mg kg^{-1}	90 days	ICR mice	Blood and BAL analysis: concentrations of pro-inflammatory cytokines (IL-1 β , TNF- α , IL-6, IL-2, Th1-type cytokines, Th2-type cytokines) and chemokines (MIP-1 α , MCP-1, and GM-CSF in BAL fluids and immunoglobulins (Ig, IgE, IgG, and IgM) in serum. Expression of genes encoding actin family cytoskeletal proteins, calcium-binding proteins, and natriuretic-related genes. Histopathological analysis of lung.	BAL: increased number of lymphocytes, GNP-engulfed macrophages and apoptotic cells; general increase in cytokine and chemokine secretion; blood: increased number of macrophages and neutrophils, and elevated production of IgG, IgM and IgA. Gene expression: elevated expression of genes related to actin family cytoskeletal proteins and calcium-binding proteins; and alteration of natriuretic-related genes expression. Histopathological analysis: presence of GNP-engulfed macrophages without pathological lesion	(119)
Single- and multi-layered GO (SLGO and MLGO) in the presence or absence of Pluronic F-127	10, 20, 40, 80 and 100 $\mu\text{g ml}^{-1}$	6 h	THP-1 cells	Cell viability, membrane integrity, cell morphology levels of cytokine and ROS production, phagocytosis, and cytometric apoptosis.	SLGO induced ROS and IL-1 β production, necrosis, and apoptosis to a lesser extent than MLGO. However, SLGO induced higher membrane damage and decrease in cell viability.	(120)
	Iv: 10 mg kg^{-1}	24 h (acute toxicity) or 10 days (chronic toxicity)	Mice	Histological analysis of lung and kidney: immunohistochemistry (IHC) for MCP-1 and TGF- β .	Both SLGO and MLGO induced acute and chronic damage to the lung and kidney in the presence or absence of Pluronic F-127.	
GO-PEG with mean thickness of 1.1 nm and lateral dimension ranged from 20 to 80 nm	It: 25 mg/kg	28 days	Balb/c mice: Age: 6–8 weeks; Weight: 18–22g	Blood circulation test; Hematologic and Biochemical marker analysis; Histopathological evaluation: trace element biodistribution observation in heart, liver spleen, lung, kidney and lymph.	Blood exposure to GO under the maximum safe starting dose caused accidental death in 1/5 <i>Macaca fascicularis</i> and 7/221 mice, while remains general amenable in others. Elevated levels of immunoglobulin E and severe lung injury were found in dead animals, suggesting the GO-induced acute anaphylactic reactions.	(121)
	4 mg/kg	90 days	<i>Macaca fascicularis</i> : Age: 4–5 years; weight: 4–5 kg			
Graphene oxide – silver nanoparticles hybrid material (GOAg)	5, 10, and 25 mg mL^{-1}	24 h	J774 and primary murine macrophages	Cell viability, apoptosis/necrosis, mitochondrial depolarization, lipid peroxidation, cytokines release (IL-1 β , TNF- α and IL-10), ratio between CD80 and CD206 macrophage populations and NO production.	GOAg induced a dose-dependent mitochondrial depolarization, apoptosis, and lipid peroxidation to J774 macrophages. However, no effects were observed on cytokines release, macrophages polarization toward M1 and NO production.	(122)
Bimetallic oxide FeWO $_x$ -PEG nanosheet (FeWO $_x$ -PEG)	0–200 $\mu\text{g ml}^{-1}$	24 h	4T1 and CT26 cells	Cell viability, internalization, ROS generation.	No significant toxicity was observed, however FeWO $_x$ -PEG could internalize <i>via</i> cell endocytosis and efficiently active OH generation and GSH depletion. No significant differences in blood chemistry were observed for FeWO $_x$ -PEG treated mice. Also, H&E staining and histology analysis showed no obvious tissue damages and adverse effects and no significative body weight changes. However, FeWO $_x$ -PEG induce strong immune responses, showed by the increase levels of IL-6, IL-12 and TNF α . Biodistribution analyses showed that the material could accumulate in liver and spleen, however, it was observed a decrease concentration after 7 and 14 days indicating the biodegradable and clearable behavior of FeWO $_x$ -PEG nanosheets.	(123)
	Toxicity: 10 mg kg^{-1} Biodistribution: 120 mg kg^{-1}		BALB/c mice	Body weight, histological analysis, blood chemistry, cytokines secretion (IL-6, IL-12 and TNF α) and biodistribution.		

(Continued)

TABLE 1 | Continued

Nanomaterial	Dose	Exposure time	<i>in vivo/in vitro</i> models	Method or endpoints	Adverse immunological effects	Ref.
FePSe ₃ @APP@CCM	0-160 µg ml ⁻¹	Viability: 6 h Cytokine secretion: 48 h	PBMC, CT26 and RAW-264.7 cells	Viability and cytokines secretion (IL-10, IL-12 and IFN-γ)	No obvious cytotoxicity was caused by the nanomaterial. However, taken together, upon NIR laser irradiation, FePSe ₃ @APP@CCM matured and activated immature DCs, enhanced the secretion of IFN-γ and IL-12, and decreased the expression and the consequent inhibitory effect of IL-10 on T cells, resulting in the enhanced immunity of T cells for killing CT26 cancer cells in the coculture system.	(124)
	10 mg kg ⁻¹	25 days	C57BL/6J mice	Body weight, blood biochemical parameters (ALT, AST, BUN, CRE, LDH and PLT), histological analysis and cytokines secretion.	No obvious abnormality, inflammation and exudation or other pathological lesions were observed. Also, it was observed the increased expression of DC-secreted cytokines, including IFN-γ and IL-12, while the level of IL-10 was found to be decreased.	
Ferrimagnetic vortex-domain iron oxide nanoring and graphene oxide (FVIOs-GO) hybrid nanoparticle	50 or 75 µg ml ⁻¹ Fe Iv: 3 mg kg ⁻¹	8 and 24 h 24 days	4T1 breast cancer cell and RAW264.7 Balb/c mice Subcutaneous 4T1 Breast Tumor Model	Cell viability, uptake, apoptosis/necrosis, ROS generation, macrophages polarization. Measurement of tumor width and length for 24 days.	Increased ROS generation and macrophage polarization to pro-inflammatory M1 phenotypes. Control group exhibited a rapid increase in the tumor volume, while FVIOs-GO group had tumor growth inhibition by 97.1%.	(125)
Borophene nanosheets (B NSs), graphene nanosheets (GR NSs) and phosphorene nanosheets (BP NSs)	Viability: 60, 80, and 100 µg ml ⁻¹ Membrane damage: 100 µg ml ⁻¹ Uptake: 200 µg ml ⁻¹	Viability: 24 h Uptake: 6 h	dTHP-1 and SC cells	Cell viability, membrane damage, cell uptake, intracellular localization, inflammatory cytokines secretion (IL-1β, IL-6, IL-8, IFN-γ and TNFα).	Corona coated 2D monoelemental nanosheets decreases cytotoxicity and cell membrane damage. For B NSs it was observed an increase in cellular uptake when the material was coronated, therefore corona may promote phagocytosis. Protein corona also stimulates the secretion of inflammatory cytokines. GR NSs and B NSs had immunoregulation behaviors only in the presence of plasma corona, while BP NSs had stronger immunoregulation behavior regardless of the absence and presence of corona.	(126)
Aggregated MoS ₂ and 2D MoS ₂ (exfoliated by lithiation or dispersed by Pluronic F87)	6.25–50 µg ml ⁻¹ 2 mg kg ⁻¹	24 h 40 h and 21 days	THP-1 and BEAS-2B cells C57BL/6 mice	Measurement of IL-8, TNF-α, and IL-1β levels BALF and lung tissue were collected for measurement of LIX, MCP-1, IL-6, TGF-β1, and PDGF-AA levels and performance of Hematoxylin and Eosin (H&E) or Masson's trichrome staining.	Aggregated MoS ₂ induced significant increases in IL-8, TNF-α, and IL-1β production, while there were significantly less effects of 2D MoS ₂ on cytokine and chemokine production. Aggregated MoS ₂ induced robust increasing in LIX, MCP-1 and IL-6 responses along with neutrophilic exudation into the BALF; while 2D MoS ₂ did not trigger cytokine or chemokine production in the lung. Histopathological changes were observed with aggregated MoS ₂ inducing focal areas of inflammation around small airways, while 2D MoS ₂ had little or no effect.	(127)
Exfoliated pristine and covalently functionalized MoS ₂	1, 10, 25, 50, 75, and 100 µg ml ⁻¹	24 h	Raw-264.7 and human monocyte-derived macrophages	Cell viability, CD86 expression and secretion of TNFα and IL6.	Cell viability was reduced only at high concentration; no variation of CD86 levels in both RAW 264.7 cells and human monocyte-derived macrophages was registered; no increase in cytokine secretion was observed for both cell lines.	(128)
Pristine MoS ₂ and PEGylated MoS ₂	10 µg ml ⁻¹	24 h	Primary mouse macrophages	Cytokine secretion (IL-6, IL-10, MCP-1, IFN-γ, TNF-α and IL-12).	Both materials significantly increased the secretion of cytokines such as IL-6, IL-12, TNF-α, IFN-γ and MCP-1. Interestingly, MoS ₂ -PEG was found to elicit stronger cytokine secretion than the pristine MoS ₂ , particularly involving IL-6, TNF-α, IFN-γ, and MCP-1.	(129)
MoS ₂ alone, MoS ₂ -PEG or MoS ₂ -PEG-CpG	0, 5, 10, 20, 30, 40 and 50 µg ml ⁻¹	48 h	RAW-264.7 cells and 4T1 cells	Cell viability, Cytokine release (TNF-α and IL-6),	MoS ₂ alone, MoS ₂ -PEG or CpG alone had no effect on cytokine release while the MoS ₂ -PEG-CpG significantly elevate the cytokine level. MoS ₂ -PEG-CpG could elevate the expression of CD86 & CD80 and the percentage of matured DCs (CD80+ CD86+ DCs) was remarkably raised to 79.8% when combined with NIR irradiation.	(130)

(Continued)

TABLE 1 | Continued

Nanomaterial	Dose	Exposure time	<i>in vivo/in vitro</i> models	Method or endpoints	Adverse immunological effects	Ref.
Protein coated with different proteins (HSA, Tf, Fg and IgG) MoS ₂ NSs	500 µg ml ⁻¹	12 and 24 h	THP-1 cells	Cellular viability, cellular uptake and cytokine release.	Protein coated MoS ₂ NSs increase viability and decrease cytoplasmic membrane damage comparing with MoS ₂ NSs. Also, the presence of a protein corona decreased the secretion of cytokines. Among the four NSs the IgG coated MoS ₂ NSs enhanced uptake and cause more inflammatory cytokines.	(31)
MoS ₂ nanosheets (100 and 500 nm)	0 – 128 µg ml ⁻¹	48 h	DC cells	Cell viability, apoptosis, ROS generation, expression of CD40, CD80, CD86 and CCR7, secretion of proinflammatory cytokines (IL-12p70, IL-6, IL-1β and TNF-α, DC homing ability.	Overall, there were no significant differences in cytotoxicity assays, however high doses could promote DC maturation as observed by the expression of CD40, CD80 and CD86 and enhanced secretion of IL-6 and TNF-α. Also, MSNs upregulate ROS generation in DCs, further promoting cytoskeletal rearrangement and promoting the local lymphoid homing ability of DCs.	(131)
Black phosphorus nanosheet (BPNSs) and black phosphorus quantum dot (BPQDs) (~300 nm)	100, 50, 25, 12.5 µg ml ⁻¹	48 h	H1299, L0-2, 293T, THP-1 cell line and SC human macrophages	Cell viability, cellular uptake (1, 3, or 6 h), intracellular localization, ROS generation, cytokines release (IL-1β, IL-6, IL-8, IL-9, IL-10, IFN-γ), NO and TNF-α generation.	A reduction of cytotoxicity was observed when BPNSs and BPQDs were coated with protein corona reduced. However, the corona facilitated the BP internalization and induced an increase in inflammatory cytokines and in ROS generation. Also, an induction of NO and TNF-α production were provoked by BP and corona coated BP.	(132)
Black phosphorus nanosheet (128 nm)	15 µg ml ⁻¹	24 h	4T1, F10, CT26 and Raw-264.7 cell lines	Cell morphology, cell expression differences, expression of the surface marker CD80 using flow cytometry, proteomic analysis, western blot analysis and immunofluorescence to analyze, expression of IL-10 (M2-related marker) and TNF-α (M1-related marker).	Corona coated black phosphorus nanosheet increase the expression of calcium signaling pathways and interact with STIM2 protein facilitating Ca ²⁺ influx promoting macrophage polarization.	(133)
Few-layer two-dimensional black phosphorous (2D BP)	10 to 500 µg.ml ⁻¹	24 h (acute toxicity) or 21 days (chronic toxicity)	SAOS-2, HOb, L929 and hMSC cell lines	Cell viability and proliferation, ROS production, immunofluorescence to analyze cell morphology, inflammatory marker expression tested by LPS to analyzed cytokine generation (IL-10 and IL-6).	Black phosphorus did not show cytotoxicity on human mesenchymal stem cells and inhibits the metabolic activity of SAOS-2 cell line while inducing both proliferation and osteogenic differentiation in HOb cell and mesenchymal stem cells. Also, the presence of BP inhibits the ALP (an early marker of osteogenesis) expression in SAOS-2 cells and induces antiproliferative and apoptotic effects by increasing the production of ROS on SAOS-2 cells. Besides, increase the inflammatory cytokine generation but inhibits proinflammatory mediators for the co-culture of SAOS-2 and HOb.	(134)
Black Phosphorus nanoflakes functionalized with TGF-β inhibitor and neutrophil membrane (NG/BP-PEI-LY)	20 µg ml ⁻¹	24 h (<i>in vitro</i>) 72 h (<i>in vivo</i>)	4T1 and HUVEC cell line BALB/c mice	Cell viability, ROS production, apoptosis, cytokine generation (IL-6 and TNF-α) Mice NIR fluorescent imaging, immunofluorescent staining of CD31 (red) and ICAM-1 (green).	NG/BP-PEI-LY induced acute inflammatory responses, cause a decrease in viability, and increase apoptosis and ROS production when laser irradiated. Besides, when laser irradiated increased the ICAM-1 expression, enhancing intracellular delivery by adhesion molecule mediated targeting.	(135)
Black Phosphorus nanosheet (BPNS) and Black Phosphorus nanocomposite (BPCP) modified with PEG and OD CpG or CpG-Cy5.5	Up to 100 µg ml ⁻¹	24 h	4T1, RAW-264.7 and Hep62	Cell viability, necroptosis, protein expression, cytokine generation (IL-6 and TNF-α) and hemocytolysis.	No obvious cytotoxicity was observed, also no significant hemolysis. For BPTT treatments it was observed that necroptosis play an important role, mediating death process in cancer cells. These results were confirmed by the expression of necroptosis-related proteins, where it was observed a significantly expression of RIP1 and RIP3. Caspase-8 and Caspase-3 levels were not significantly changed.	(136)

(Continued)

TABLE 1 | Continued

Nanomaterial	Dose	Exposure time	<i>in vivo/in vitro</i> models	Method or endpoints	Adverse immunological effects	Ref.
	2 mg/kg	Up to 16 days	BALB/c mice	Biodistribution, expression of immune factors (FOXP3, IL-2, TNF- α and INF- γ), histological analysis, hematological toxicity.	No body weight loss and no systemic toxicity were observed. Also, no tissue damage and blood physiological indicators were within normal range. After BPTT treatments the immune responses were activated as observed by detection of T lymphocytes and various immune cytokines.	
DSPE-PEG coated Tao nanosheet (92.5 nm)	1 mg ml ⁻¹	30 days	C57 mice	Body weight, biodistribution, immunogenicity, hematological toxicity, liver and spleen histopathology, oxidative stress response.	DSPE-PEG coated TiO ₂ nanosheet cause a decrease in body weight after 14 to 30 days of the injection, also, it was observed a that the particles were accumulated in liver and cause liver toxicity by inducing oxidative stress. Besides, an obvious decrease in HTC and significant increase in MCH and MCHC indicate that the particles may induce blood system damage.	(137)
Two-Dimensional Core – Shell MXene@Gold Nanocomposites	<i>In vitro</i> : 3.1 to 100 μ g ml ⁻¹ <i>In vivo</i> : 20 mg kg ⁻¹	24 h 30 days	4T1 cell line Balb/c mice	Cell viability, immunohistochemistry and immunofluorescence staining. Body weight and biodistribution.	Overall, the particle did not show apparent cytotoxicity, and no toxic side effect was observed in mice after 30 days of injection. No height loss and no notable abnormality on major organs were observed.	(138)
2D titanium nanosheets (TINS) and polyethylene glycol coated titanium nanosheets (TINS-PEG)	<i>In vitro</i> : 10-100 ppm <i>In vivo</i> : 5 mg kg ⁻¹	4 h 19 days	A1 cell line, J774A.1 cell line and SMMC-7721. Balb/c mice	Cell viability. Histopathology, body weight, biodistribution and hematological toxicity.	TINS and TINS-PEG did not significantly affect cell viability. Any significant differences on mice body weight, no histological abnormalities, and no impact on hematological parameters, indicating no inflammation and other negative impact on blood and organs was observed.	(139)
PEGylated molybdenum dichalcogenides (MoS ₂ -PEG), tungsten dichalcogenides (WS ₂ -PEG) and titanium dichalcogenides (TiS ₂ -PEG) nanosheets	<i>In vitro</i> : 25 – 200 μ g ml ⁻¹ <i>In vivo</i> : 10 mg kg ⁻¹	24 h up to 60 days post injection	RAW-264.7, 4T1 and 293T. Balb/c mice.	Cell viability and ROS generation. biodistribution, hematological toxicity, biochemical parameters (ALP, ALT, AST and BUN) and histopathology.	No significant <i>in vitro</i> cytotoxicity was observed for all the three types of PEG functionalized TMDCs. The materials show dominate accumulation in reticuloendothelial systems (RES) such as liver and spleen after intravenous injection. Also, no significant results were observed for the analyzed biochemical and hematological parameters and no obvious sign of abnormality, such as inflammation, was noticed in all examined major organs.	(140)
Two-dimensional polyethylene glycol modified TiS ₂ nanosheets (TiS ₂ -PEG)	<i>In vitro</i> : 0.0015 – 0.1 mg ml ⁻¹ <i>In vivo</i> : 20 mg kg ⁻¹	24 h 60 days	4T1 cell and Balb/c mice	Cell viability <i>In vivo</i> toxicity, histopathology.	No significant cytotoxicity of TiS ₂ -PEG was observed. No histological abnormalities and no obvious toxicity to Balb/c mice was observed.	(141)
BSA coated 2D silicene nanosheets (SNSs-BSA)	<i>In vitro</i> : 12.5 – 200 μ g ml ⁻¹ <i>In vivo</i> : 20 mg kg ⁻¹	24 h 4 weeks	4T1 and U87 cell lines Kunming mice and Balb/c mice	Cell viability Body weight, histopathology, hematological toxicity, biochemical parameters (ALT, AST, ALP, urea, CREA, and UA).	SNSs-BSA exhibit insignificant effect on cell viability of either 4T1 or U87 cancer cells. In a four-week duration, the mice present no significant abnormality, body weight differences, and no significant behavioral alterations. The histological observations of major organs showed no significant acute pathological toxicity. Furthermore, hematological parameters showed no obvious sign of abnormalities indicating that the SNSs-BSA induce negligible renal and hepatic toxicity in mice model.	(142)
Poly (vinylpyrrolidone)-encapsulated Bi ₂ Se ₃ nanosheets (diameter 31.4 nm and thickness 1.7 nm)	<i>In vitro</i> : 5 – 200 ppm <i>In vivo</i> : 27 – 1168 mg kg ⁻¹	48 h 14 days	MCF7 cell line Balb/c mice	Cell viability <i>in vivo</i> toxicity and biodistribution.	It was not observed any cytotoxicity effects caused by Bi ₂ Se ₃ nanosheets. At the dose of 750 or less no mice mortality nor any reaction was observed. The nanomaterial mainly accumulated in liver, spleen and kidney, however, the concentration decreases with time.	(143)

(Continued)

TABLE 1 | Continued

Nanomaterial	Dose	Exposure time	<i>in vivo/in vitro</i> models	Method or endpoints	Adverse immunological effects	Ref.
Pd nanosheets (diameter ranging from 5 to 80 nm)	<i>In vitro</i> : up to 100 $\mu\text{g mL}^{-1}$	24 h	NIH-3T3, 4T1, Raw-264.7, QSG-7701 and QGY-7703 cell lines	Cell viability, mitochondrial membrane depolarization and ROS generation.	Pd nanosheets have no effect on cell viability, apoptosis, ROS generation, or mitochondrial depolarization.	(144)
	<i>In vivo</i> : 10 mg kg^{-1}	30 days	Balb/c mice	Biodistribution, blood chemistry and hematology analysis and histopathology.	The <i>in vivo</i> results show that the particle is primarily trapped by reticuloendothelial system (RES). Also, no significant hepatotoxicity was induced by Pd nanosheets of different sizes. The activity of ALP, ALT, AST and BUN observed was within normal range and no apparent histopathological abnormalities or lesions were observed in any major organ.	
PEGylated ultrathin boron nanosheets (B-PEG NSs)	25 to 500 $\mu\text{g mL}^{-1}$	48 h	HeLa, PC3, MCF7, and A549	Cell viability, ROS generation.	No significant cytotoxicity was observed for B-PEG NSs. However, when exposed to an 808 nm NIR laser (1 W cm^{-2}) for 5 min it was noticed a strong concentration-dependent cytotoxicity. Also, when the B-PEG NSs were combined with DOX and NIR laser irradiation, over 95% of the cells died at a DOX concentration of 100 $\mu\text{g mL}^{-1}$.	(89)
	5.3 mg kg^{-1}	24 h	Mice	Body weight, histopathology, hematological toxicity (HGB, WBC, RBC, MCV, MCHC, PLT, MCH, HCT, Cr, NEU, LYM, MPV), biochemical parameters (ALP, AST, BUN and ALT) and cytokine generation (TNF- α , IL-6, IFN- γ , and IL-12+P40)	No obvious side effects were noted, also the levels of TNF- α , IL-6, IFN- γ , and IL-12+P40 were similar to those in the PBS control group indicating that B-PEG NSs did not induce obvious cytokine response. Compared with the control group, there is no statistically significant difference of the NSs-treated groups with PBS-treated groups in all the parameters, no obvious induction on cytokine response, no change in biochemical parameter and no hematological toxicity, therefore, B-PEG NSs do not cause obvious infection and inflammation in the treated mice. Moreover, no noticeable signal of inflammation or tissue damage was observed in major organs.	

¹Ip, intraperitoneal; ²Lung, oropharyngeal aspiration; ³It, intratail.

GO-PEG, poly-(ethylene glycol)-functionalized GO; PG-FMN, flavin mononucleotide-stabilized pristine graphene; GO-NH₂, aminated GO; GO-PAM, poly(acrylamide)-functionalized GO; GO-PAA, poly(acrylic acid)-functionalized GO; PEG, polyethylene glycol; DSPE-PEG, N-(carbonyl-methoxypolyethyleneglycol 5000)-1,2-distearoyl-sn-glycero-3-phosphoethanolamine; HSA, human serum albumin; Tf, transferrin; Fg, fibrinogen; IgG, immunoglobulin G; NSs, Nanosheets; ALP, aspartate aminotransferase; ALT, alanine aminotransferase; LDH, lactate dehydrogenase; BUN, blood urea nitrogen; CRE, creatinine; lactate dehydrogenase; PLT, platelet; NO, nitric oxide; IHC, immunohistochemistry; Nuclear NMR, magnetic resonance spectroscopy; TCA, tricarboxylic acid cycle; PVP, polyvinyl chloride; LPS, lipopolysaccharide; Rho/ROCK, Rho-associated protein kinase; RBC, red blood cells; WBC, white blood cells; MMP, mitochondrial membrane potential; MAPKs, mitogen-activated protein kinase; ERK, extracellular signal-regulated kinase; JNK, c-Jun N-terminal kinase; GSH, glutathione; BALF, bronchoalveolar lavage fluid; LYM, lymphocytes; MPV, mean platelets volume; HTC, hematocrit count; HGB, hemoglobin; MCV, mean volume cell; MCH, mean cell hemoglobin; MCHC, MCH concentration; NEU, neutrophil count; DOX, doxorubicin; NIR, near infrared light; UA, uric acid; CpG, cytosine-phosphate-guanine; BPTT, black phosphorus based photothermal therapy; TMDC, transition metal dichalcogenides.

demonstrated that small MoS₂ nanoflakes can penetrate the macrophage membrane, and that the PEG chain on PEG-MoS₂ lead to a prolonged passage throughout the membrane. Such a result might explain why PEG-MoS₂ triggers sustained more stimulation of macrophages than pristine MoS₂.

Other types of functionalization have also been studied in respect to their biocompatibility to immune cells. For instance, Zhi et al. (112) reported that the polyvinylpyrrolidone (PVP) coating of GO has exhibited lower immunogenicity when compared with pristine GO in relation to the inducing differentiation and maturation of dendritic cells (DCs), provoking a delaying in apoptotic process of T lymphocytes and the anti-phagocytosis ability against macrophages.

Surface chemistry has also been shown to influence on the immunotoxicity of 2D materials. Gurunathan et al. (114)

reported that both GO and reduced GO (rGO) induced a dose-dependent loss of cell viability and proliferation, cell membrane damage, a loss of mitochondrial membrane potential, a decreased level of ATP, a redox imbalance, and an increased secretion of various cytokines and chemokines (IL1- β , TNF- α , GM-CSF, IL-6, IL-8, and MCP-1) by THP-1 cells. However, to all these toxic effects the rGO presented a significantly worse response compared to GO. In a previous study, Yan et al. (115) showed that different oxidation degrees resulted in the toxicity of monocytes *via* different signaling pathways, with GO nanoplatelets (GONPs) inducing the expression of antioxidative enzymes and inflammatory factors, whereas the reduced GO nanoplatelets (rGONPs) activated the NF- κ B pathway. The contradictory results between these two studies, in relation to cytokine and chemokine expression, may

be due to differences in the GBMs studied (i.e. GO sheets *versus* GO nanoplatelets), and they raise the need for further investigation concerning the effects of the oxidative degree of GBMs on immune cells.

In order to investigate the pristine graphene effects *in vitro* (THP-1 cell line) and *in vivo* (C57BL/6 strain mice), Schinwald et al. (118) have assessed the impacts of the shape of graphene nanoplatelets (GNPs) on their inflammatory potential. This large few-layer graphene presented as inflammogenic both *in vitro* and *in vivo*, which was attributed to its large size that led to frustrated phagocytosis. The authors highlighted that the potential hazard of GNPs could be minimized by producing GNPs small enough to be phagocytosed by macrophages. Moreover, the number of GO layers has been shown to affect its immunotoxicity, in which single-layer GO (SLGO) caused a more pronounced decrease in cell viability due to membrane damage of THP-1 cells, while multi-layer GO (MLGO) induced higher reactive oxygen species (ROS) and IL-1 β production, leading to necrosis and apoptosis (120). In addition, the histological animal analysis revealed that SLGO and MLGO induced acute and chronic damage to the lungs and kidneys in the presence or absence of Pluronic F-127 (120).

Another important parameter, when approaching nanomaterial biosafety, is colloidal stability. Aggregation can influence the immunological response as observed by Wang et al. (127), when compared the toxicological profile of 2D MoS₂ versus aggregated MoS₂ in lung cells and mice. In their *in vitro* evaluation, in THP-1 and BEAS-2B cells, they found that aggregated MoS₂ induces strong proinflammatory and profibrogenic responses, while 2D MoS₂ have little or no effect. In agreement with *in vitro* results, an acute toxicity study *in vivo* showed that aggregated MoS₂ induced an acute lung inflammation, while 2D MoS₂ had no or a slight effect.

To increase the stability of 2D materials, studies have shown that proteins can be used as a dispersant agent. Lin et al. (142) studied silicene nanosheets modified with a bovine albumin serum protein corona (SNSs-BSA) and observed a significant increase in the colloidal stability in several physiological media (0.9% saline, phosphate buffered saline and Dulbecco's modified Eagle medium). Furthermore, SNSs-BSA did not cause significant toxicity *in vitro* neither significant acute toxicity *in vivo*. Only meaningless hematological changes were observed during the treatment duration, and no significant inflammation or infection were caused by the SNSs-BSA.

It is imperative that in a physiological environment, the nanomaterials will interact with biomolecules, forming a complex biomolecular corona. Those biomolecules (e.g., proteins, lipids, carbohydrates) can change the identity of the nanomaterials and influence their interaction with biological systems, causing an increase or decrease in internalization, toxicity, and biocompatibility as well as in colloidal stability over time. Thus, the biotransformation of nanomaterials in a physiological environment is an important parameter to be studied (146). The most common and highly studied component of biomolecular corona is the protein corona. In

this sense, Mo et al. (132) studied the effect of the human plasma protein corona on the cytotoxicity of BP nanosheets and BP quantum dots (BPQDs) observing a reduction in cell viability for both nanomaterials when coated with proteins. However, protein corona facilitated BP nanosheet internalization and induced an increase in inflammatory cytokines (IL-1 β , IL-6, IL-8 and IFN- γ) and in ROS generation. Besides, it was observed that protein corona coated BP caused an induction on the nitric oxide (NO) and tumour necrosis factor. Further, Mo et al. (133) studied the effect of the human plasma protein corona in BP toxicity, and observed an increased macrophage polarization due to the adsorption of opsonins present in the plasma, increasing the uptake of BP and the interaction with stromal interaction molecule 2 (STIM2) protein facilitating Ca²⁺ influx.

Similarly, Han et al. (126) studied the effect of plasma corona-coated 2D monoelemental nanosheets and observed that the protein corona decreases cytotoxicity and cell membrane damage for borophene, phosphorene, and graphene nanosheets. The corona coating induced the secretion of inflammatory cytokines (IL-1 β , IL-6, IL-8, and IFN- γ) for all three materials. Also, for BNNs, it was observed an increase in cellular uptake when the material was coronated, and therefore, the corona may promote phagocytosis. Baimanov et al. (31) also investigated the effect of four different blood protein coronas (human serum albumin (HSA), transferrin (Tf), fibrinogen (Fg), and immunoglobulin G (IgG) corona) on cell viability, uptake, and pro-inflammatory effects of MoS₂ nanosheets (NSs) in the macrophages cell line. Their results demonstrate that blood proteins contribute to uptake and inflammatory effects, as protein coated MoS₂ NSs increase cell viability and decrease cytoplasmic membrane damage when compared to non-coated MoS₂ NSs. Besides, it was observed that the type of protein influences cytokine secretion, as IgG-coated MoS₂ NSs causes more inflammatory cytokine secretion (TNF- α , IL-6 and IL-1 β). The highest proportion of β -sheets on IgG led to fewer secondary structure changes on MoS₂ NSs, facilitating uptake and producing a stronger pro-inflammatory response in macrophages due to the recognition of an MoS₂ NSs-IgG complex by Fc gamma receptors and the subsequent activation of the NF- κ B pathways. Another interesting finding is that in a serum-containing medium, cellular uptake of MoS₂ NSs-protein complexes was higher than that in a serum-free medium. Also, the MoS₂ NSs-Fg, and MoS₂ NSs-serum complexes had similar results in serum-free conditions and different results in a serum-containing medium, suggesting the formation of the protein corona layer above the previously formed MoS₂ NSs-protein complexes. Those studies can help to elucidate the mechanisms in which protein corona can affects the toxicity of 2D materials.

One important ability of the immune system is the innate immune memory, where cells from the innate immune system react to secondary stimulus, which mostly includes an increased or decreased production of inflammation-related factors (147). With regard to 2D materials studies, there is yet a little research on this topic. Liu et al. (148) functionalize GO with lentinan (LNT) and observed that GO-LNT was able to promote macrophage activation by NF- κ B and TLR signaling pathway,

as well as enhance antigen protein processing after initial contact with macrophage. Moreover, the efficiency of this material was investigated, as a vaccine adjuvant for ovalbumin (OVA), in this sense GO-LNT induced robust long-term OVA-specific antibody responses due to the prolonged release of OVA. Besides this, GO-LNT was able to sustain a long-term immune response because it facilitated the uptake and slowed the release rate of antigen in macrophage. Further, Lebre et al. (149), demonstrated that pristine graphene can promote the innate immune training, enhancing the secretion of IL-6 and TNF- α and a decrease in IL-10 after toll-like receptor ligand stimulation 5 days after graphene exposure, indicating that pristine graphene can activate the immune innate memory.

Immune cells, such as macrophages and neutrophils, are one of the first line of defense of the immune system; they are capable of engulf the foreign material (or pathogen), degrading it and producing cytokines to enhanced the immune response (150). The uptake of 2D materials by immune system cells have been reported in various studies (31, 109, 115, 126, 132); however, there are few studies that address the degradation of those materials after internalization. Mukherjee et al. (151) studied the degradation of large and small GO by neutrophils and observed that not only both GO be degraded by neutrophils but also that the product of the degradation was non-toxic to human cells. Similarly, Moore et al. (152) studied the degradation of few-layer MoS₂ in human macrophage-like cells and observed that internalization occurred following 4 h of exposure and after 24 h the *in vitro* degradation of the material was confirmed, which occurred within lipidic vesicles and associated with enzymatic regions containing lysozyme.

As presented above, 2D nanomaterials may have an inflammogenic potential and immunotoxicity, which may impair their successful clinical translation; however, the immunological system activation can also be useful for theragnostic purposes. This application uses the immune responses to protect the body and eliminate cancer cells. The advantage of immunotherapy is that it engages the immune system to kill tumor cells without damaging healthy cells, additionally, it may induce immunological memory, causing long-lasting protection (153).

Nanoinformatics Approaches Toward Immunosafety-by-Design

In materials science, theory, computational modeling and informatics have a substantial role in accelerating and discovering new materials with interesting properties and applications (154–156). Due to the growing interest in 2D nanomaterials, computational approaches are extensively used in the discovery, development and application of these materials by detailed study of their structure/property relationships (156–158).

The nano-bio interface phenomena are directly related to the physicochemical properties of nanomaterials. However, tracing general correlations and delineating predictive models of nanomaterials biological effects remains challenging. Some issues include the complexity of nano-bio interactions, nanomaterials structural heterogeneity, lack of standard methodologies, absence

of systematic studies and low-quality nanomaterial characterization (159–161). In this context, computational methods have been incorporated into the nanotoxicology field to support the understanding of the nano-bio interface to enable the development of safe-by-design principles applied to nanomaterials (162, 163). Theoretical modeling (i.e., molecular dynamics, density functional theory) enables precise control of critical parameters of the nanomaterials surface to study their individual effects in nano-bio interactions, providing mechanistic knowledge (164–166). On the other hand, machine learning (ML) techniques are used to assess datasets of nanomaterials biological outcomes in order to find patterns and correlations between physicochemical properties and biological effects, often undetectable through other types of analysis (167–169).

Applications of data-driven strategies include data filling, grouping, and predictive modeling. Quantitative nanostructure–activity relationships (QNAR) consist of the main strategy to delineate prediction models based on correlations between nanomaterial structural characteristics to their properties and biological activities (170, 171). It is based on the assumption that nanomaterials in their properties present similar biological effects. Diverse algorithms can be used in QNAR models, including support vector machine (172), artificial neural network (173), and decision trees (174), among others, and depending of the level of algorithms interpretability may enable the outline of causal relationships.

The scarcity of quality data and comprehensive databases is the major bottleneck in the application of ML to predict nanomaterials immune reactions (175, 176). Data-driven strategies have been making important advances in modeling biological phenomena that have potential usage to evaluate nano-immune interactions, such as predicting biomolecular corona compositions (177–181), and nanomaterials and cell interactions (e.g., cell uptake, cytotoxicity, membrane integrity, oxidative stress) (182–185). Furthermore, the exploration of omics approaches (e.g., genomics, transcriptomics, and metabolomics) has promoting the development of ML models to process the complex data generated by these techniques and enables a better understanding of the molecular mechanisms of nanomaterials adverse effects in a systemic context, defining and predicting adverse outcome pathways (186–189). The omics' potential of data generation is demonstrated by Kinet et al. (190), who were able to connect immune responses to observed transcriptomic alterations in mouse airway exposed to 28 engineered nanomaterials. Together with cytological and histological analyses (imaging processing), they generated an extensive *in vivo* data set of nanomaterial adverse effects.

Allied with quality data infrastructure and processing, computational methods are sizeable to deal with complexity of nano-bio interface to assess and model the toxicity of nanomaterials in a variety of environments (163, 191–194). To support safe-by-design approaches, international efforts have been made to provide data integration and sharing, modeling tools, standard protocols, and ontologies, to ensure Findable, Accessible, Interoperate, and Reusable (FAIR) data (195, 196). For example, European projects, such as NanosolveIT and NanoCommons, and

more recently CompSafeNano are initiatives facing on this direction (164, 165, 197, 198). In accordance with these initiatives, Gazzi et al. (199) recently presented the nanoimmunity-by-design concept developed inside G-IMMUNOMICS and CARBO-IMmap projects, which aim to bridge the knowledge gaps in the immune characterization of carbon-based materials, integrating data-driven methodologies which are extendable to other 2D materials.

CONCLUSIONS AND FUTURE PERSPECTIVES

Two-dimensional materials are key elements for nanoscience and innovation in energy, health, and the environment. This can lead to a broad range of technological applications, especially nano-imaging, which has been growing exponentially in recent years. The wide number of 2D materials with different physicochemical properties make immunotoxicity and safety evaluation a challenge. There are therefore still gaps and controversial data in the literature. For example, within the same material category (i.e., graphene oxide) different properties were observed that might affect immunological and toxicological responses. It is imperative to evaluate the biological effects of biomolecular corona formation on 2D materials at nanobiointerfaces. Only by the identification of these material properties (intrinsic and extrinsic) and an integrated understanding on how they may influence its immunological response, we can manage immunotoxicity/biocompatibility and then benefit from their unique properties for many applications. Furthermore, it is very important to highlight the critical influence of endotoxin contamination prior immunological studies and toxicity testing. Special attention on this topic will avoid misinterpretation of immunosafety results involving 2D materials (148). In addition, it is important to advance in the understanding of the links between nanomaterials and the immune system across environmental species; this being a future challenge for immunosafety research associated with 2D materials (200). Nanoinformatics and computational modeling will have a decisive role on immunotoxicological studies with nanomaterials toward the practical implementation of immunosafety-by-design. However,

it is very important to develop harmonized protocols, ontologies, and public databases to facilitate and promote a global research community for the collaboration and an exchange of knowledge in this field, focusing efforts on FAIR data principles.

AUTHOR CONTRIBUTIONS

All authors listed have made a substantial, direct and intellectual contribution to the work, and approved it for publication. GS and LFr: literature research, data curation, writing, and editing. RP, LFo, and MM: literature research and writing. DM, AF, and OA: funding acquisition, supervision, project administration, and writing. All authors contributed to the article and approved the submitted version.

FUNDING

This work was funded by the Sao Paulo Research Foundation (FAPESP, grant no. 18/25103-0; 17/02317-2; 14/50906-9), the National Council for Scientific and Technological Development (CNPq, grant no. 315575/2020-4; 301358/2020-6), and the Coordination for the Improvement of Higher Education Personnel (CAPES, Finance code 001).

ACKNOWLEDGMENTS

The authors thank the National System of Laboratories in Nanotechnologies (SisNANO/MCTI), the National Institute for Research and Development in Complex Functional Materials (INCT-Inomat) and the National Institute for Research and Development in Carbon nanomaterials (INCT-NanoCarbono).

SUPPLEMENTARY MATERIAL

The Supplementary Material for this article can be found online at: <https://www.frontiersin.org/articles/10.3389/fimmu.2021.689519/full#supplementary-material>

REFERENCES

- Nicolosi V, Chhowalla M, Kanatzidis MG, Strano MS, Coleman JN. Liquid Exfoliation of Layered Materials. *Sci* (80-) (2013) 340:1226419–1226419. doi: 10.1126/science.1226419
- Hu T, Mei X, Wang Y, Weng X, Liang R, Wei M. Two-Dimensional Nanomaterials: Fascinating Materials in Biomedical Field. *Sci Bull* (2019) 64:1707–27. doi: 10.1016/j.scib.2019.09.021
- Novoselov KS, Geim AK, Morozov SV, Jiang D, Zhang Y, Dubonos SV, et al. Electric Field in Atomically Thin Carbon Films. *Sci* (80-) (2004) 306:666–9. doi: 10.1126/science.1102896
- Hao S, Zhao X, Cheng Q, Xing Y, Ma W, Wang X, et al. A Mini Review of the Preparation and Photocatalytic Properties of Two-Dimensional Materials. *Front Chem* (2020) 8:582146. doi: 10.3389/fchem.2020.582146
- Mohammadpour Z, Majidzadeh-a K. Applications of Two-Dimensional Nanomaterials in Breast Cancer Theranostics. *ACS Biomater Sci Eng* (2020) 6(4):1852–73. doi: 10.1021/acsbomaterials.9b01894
- Rohaizad N, Mayorga-Martinez CC, Fojtů M, Latiff NM, Pumera M. Two-Dimensional Materials in Biomedical, Biosensing and Sensing Applications. *Chem Soc Rev* (2021) 50:619–57. doi: 10.1039/d0cs00150c
- Bolotsky A, Butler D, Dong C, Gerace K, Glavin NR. Two-Dimensional Materials in Biosensing and Healthcare: From In Vitro Diagnostics to Optogenetics and Beyond. *ACS Nano* (2019) 13:9781–810. doi: 10.1021/acsnano.9b03632
- Samori P, Feng X, Palermo V. Introduction to 'Chemistry of 2D Materials: Graphene and Beyond.' *Nanoscale* (2020) 12:24309–10. doi: 10.1039/d0nr90263b
- Ostadoshehin A, Guo J, Simeski F, Ihme M. Functionalization of 2D Materials for Enhancing OER/ORR Catalytic Activity in Li-oxygen Batteries. *Commun Chem* (2019) 2:1–11. doi: 10.1038/s42004-019-0196-2

10. Och M, Martin M, Dlubak B, Mattevi C, Martin M, Martin M. Synthesis of Emerging 2D Layered Magnetic Materials. *Nanoscale* (2021) 13:2157–80. doi: 10.1039/d0nr07867k
11. Tao W, Ji X, Zhu X, Li L, Wang J, Zhang Y, et al. Two-Dimensional Antimonene-Based Photonic Nanomedicine for Cancer Theranostics. *Adv Mater* (2018) 30:1–11. doi: 10.1002/adma.201802061
12. Tao W, Zhu X, Yu X, Zeng X, Xiao Q, Zhang X, et al. Black Phosphorus Nanosheets as a Robust Delivery Platform for Cancer Theranostics. *Adv Mater* (2017) 29:1–9. doi: 10.1002/adma.201603276
13. Ares P, Palacios JJ, Abellán G, Gómez-Herrero J, Zamora F. Recent Progress on Antimonene: A New Bidimensional Material. *Adv Mater* (2018) 30:1–27. doi: 10.1002/adma.201703771
14. Wang H, Wang X, Xia F, Wang L, Jiang H, Xia Q, et al. Black Phosphorus Radio-Frequency Transistors. *Nano Lett* (2014) 14:6424–9. doi: 10.1021/nl5029717
15. Ugeda MM, Bradley AJ, Shi SF, Da Jornada FH, Zhang Y, Qiu DY, et al. Giant Bandgap Renormalization and Excitonic Effects in a Monolayer Transition Metal Dichalcogenide Semiconductor. *Nat Mater* (2014) 13:1091–5. doi: 10.1038/nmat4061
16. Huang C, Wu S, Sanchez AM, Peters JJP, Beanland R, Ross JS, et al. Lateral Heterojunctions Within Monolayer MoSe₂-WSe₂ Semiconductors. *Nat Mater* (2014) 13:1096–101. doi: 10.1038/nmat4064
17. Abo El-Reesh GY, Farghali AA, Taha M, Mahmoud RK. Novel Synthesis of Ni/Fe Layered Double Hydroxides Using Urea and Glycerol and Their Enhanced Adsorption Behavior for Cr(VI) Removal. *Sci Rep* (2020) 10:1–20. doi: 10.1038/s41598-020-57519-4
18. Zhu C, Du D, Lin Y. Graphene and Graphene-Like 2D Materials for Optical Biosensing and Bioimaging: A Review. *2D Mater* (2015) 2:32004. doi: 10.1088/2053-1583/2/3/032004
19. Eom S, Choi G, Nakamura H, Choy J-H. 2-Dimensional Nanomaterials With Imaging and Diagnostic Functions for Nanomedicine; A Review. *Bull Chem Soc Jpn* (2020) 93:1–12. doi: 10.1246/bcsj.20190270
20. Wang X, Cheng L. Multifunctional Two-Dimensional Nanocomposites for Photothermal-Based Combined Cancer Therapy. *Nanoscale* (2019) 11:15685–708. doi: 10.1039/C9NR04044G
21. Cai X, Liu X, Jiang J, Gao M, Wang W, Zheng H, et al. Molecular Mechanisms, Characterization Methods, and Utilities of Nanoparticle Biotransformation in Nanosafety Assessments. *Small* (2020) 1907663:1–19. doi: 10.1002/smll.201907663
22. Fadeel B, Bussy C, Merino S, Vázquez E, Flahaut E, Mouchet F, et al. Safety Assessment of Graphene-Based Materials: Focus on Human Health and the Environment. *ACS Nano* (2018) 12:10582–620. doi: 10.1021/acsnano.8b04758
23. Chetwynd AJ, Wheeler KE, Lynch I. Best Practice in Reporting Corona Studies: Minimum Information About Nanomaterial Biocorona Experiments (Minbe). *Nano Today* (2019) 28:100758. doi: 10.1016/j.nantod.2019.06.004
24. Ma B, Martin C, Kurapati R, Bianco A. Degradation-by-Design: How Chemical Functionalization Enhances the Biodegradability and Safety of 2D Materials. *Chem Soc Rev* (2020) 49:6224–47. doi: 10.1039/c9cs00822e
25. Ganguly P, Breen A, Pillai SC. Toxicity of Nanomaterials: Exposure, Pathways, Assessment, and Recent Advances. *ACS Biomater Sci Eng* (2018) 4:2237–75. doi: 10.1021/acsbomaterials.8b00068
26. Orecchioni M, Bedognetti D, Newman L, Fuoco C, Spada F, Hendrickx W, et al. Single-Cell Mass Cytometry and Transcriptome Profiling Reveal the Impact of Graphene on Human Immune Cells. *Nat Commun* (2017) 8(1):1–14. doi: 10.1038/s41467-017-01015-3
27. Kämpfer AAM, Busch M, Schins RPF. Advanced In Vitro Testing Strategies and Models of the Intestine for Nanosafety Research. *Chem Res Toxicol* (2020) 33:1163–78. doi: 10.1021/acs.chemrestox.0c00079
28. Cronin JG, Jones N, Thornton CA, Jenkins GJS, Doak SH, Clift MJD. Nanomaterials and Innate Immunity: A Perspective of the Current Status in Nanosafety. *Chem Res Toxicol* (2020) 33:1061–73. doi: 10.1021/acs.chemrestox.0c00051
29. Franqui LS, De Farias MA, Portugal RV, Costa CAR, Domingues RR, Souza Filho AG, et al. Interaction of Graphene Oxide With Cell Culture Medium: Evaluating the Fetal Bovine Serum Protein Corona Formation Towards In Vitro Nanotoxicity Assessment and Nanobiointeractions. *Mater Sci Eng C* (2019) 100:363–77. doi: 10.1016/j.msec.2019.02.066
30. Cao M, Cai R, Zhao L, Guo M, Wang L, Wang Y, et al. Molybdenum Derived From Nanomaterials Incorporates Into Molybdenum Enzymes and Affects Their Activities In Vivo. *Nat Nanotechnol* (2021) 1–9. doi: 10.1038/s41565-021-00856-w
31. Baimanov D, Wu J, Chu R, Cai R, Wang B, Cao M, et al. Immunological Responses Induced by Blood Protein Coronas on Two-Dimensional Mos 2 Nanosheets. *ACS Nano* (2020) 14:5529–42. doi: 10.1021/acsnano.9b09744
32. Ede JD, Lobaskin V, Vogel U, Lynch I, Halappanavar S, Doak SH, et al. Translating Scientific Advances in the AOP Framework to Decision Making for Nanomaterials. *Nanomaterials* (2020) 10:1–22. doi: 10.3390/nano10061229
33. Chen C, Leong DT, Lynch I. Rethinking Nanosafety: Harnessing Progress and Driving Innovation. *Small* (2020) 16:2–5. doi: 10.1002/smll.202002503
34. Miernicki M, Hofmann T, Eisenberger I, Von Der KF, Praetorius A. Legal and Practical Challenges in Classifying Nanomaterials According to Regulatory Definitions. *Nat Nanotechnol* (2019) 14(3):208–16. doi: 10.1038/s41565-019-0396-z
35. Shatkin JA. The Future in Nanosafety. *Nano Lett* (2020) 20:1479–80. doi: 10.1021/acs.nanolett.0c00432
36. Varsou D, Afantitis A, Tsoumanis A, Melagraki G, Sarimveis H, Valsamijones E. Nanoscale Advances A Safe-by-Design Tool for Functionalised Nanomaterials Through the Enalos Nanoinformatics. *Nanoscale Adv* (2019) 1:706–18. doi: 10.1039/c8na00142a
37. Singh AV, Maharjan RS, Kanase A, Siewert K, Rosenkranz D, Singh R, et al. Machine-Learning-Based Approach to Decode the Influence of Nanomaterial Properties on Their Interaction With Cells. *ACS Appl Mater Interfaces* (2021) 13:1943–55. doi: 10.1021/acsaami.0c18470
38. Sturla SJ, Boobis AR, FitzGerald RE, Hoeng J, Kavlock RJ, Schirmer K, et al. Systems Toxicology: From Basic Research to Risk Assessment. *Chem Res Toxicol* (2014) 27:314–29. doi: 10.1021/tx400410s
39. Li B, Wu Y, Li N, Chen X, Zeng X, Arramel, et al. Single-Metal Atoms Supported on MBenes for Robust Electrochemical Hydrogen Evolution. *ACS Appl Mater Interfaces* (2020) 12:9261–7. doi: 10.1021/acsaami.9b20552
40. Wang Y, Polavarapu L, Liz-Marzán LM. Reduced Graphene Oxide-Supported Gold Nanostars for Improved SERS Sensing and Drug Delivery. *ACS Appl Mater Interfaces* (2014) 6:21798–805. doi: 10.1021/am501382y
41. Yin W, Yan L, Yu J, Tian G, Zhou L, Zheng X, et al. High-Throughput Synthesis of Single-Layer MoS₂ Nanosheets as a Near-Infrared Photothermal-Triggered Drug Delivery for Effective Cancer Therapy. *ACS Nano* (2014) 8:6922–33. doi: 10.1021/nn501647j
42. Garcia-Gallastegui A, Iruretagoyena D, Gouvea V, Mokhtar M, Asiri AM, Basahel SN, et al. Graphene Oxide as Support for Layered Double Hydroxides: Enhancing the CO₂ Adsorption Capacity. *Chem Mater* (2012) 24:4531–9. doi: 10.1021/cm3018264
43. Warner JH, Rummeli MH, Bachmatiuk A, Büchner B. Atomic Resolution Imaging and Topography of Boron Nitride Sheets Produced by Chemical Exfoliation. *ACS Nano* (2010) 4:1299–304. doi: 10.1021/nn901648q
44. Huang Y, Sutter E, Sadowski JT, Cotlet M, Monti OLA, Racke DA, et al. Tin Disulfide—an Emerging Layered Metal Dichalcogenide Semiconductor: Materials Properties and Device Characteristics. *ACS Nano* (2014) 8:10743–55. doi: 10.1021/nn504481r
45. Naguib M, Mashtalir O, Carle J, Presser V, Lu J, Hultman L, et al. Two-Dimensional Transition Metal Carbides. *ACS Nano* (2012) 6:1322–31. doi: 10.1021/nn204153h
46. Shwetharani R, Kapse S, Thapa R, Nagaraju DH, Balakrishna RG. Dendritic Ferroselite (FeSe₂) With 2D Carbon-Based Nanosheets of rGO and G-C₃N₄s Efficient Catalysts for Electrochemical Hydrogen Evolution. *ACS Appl Energy Mater* (2020) 3:12682–91. doi: 10.1021/acsaem.0c02619
47. Wang Z, Li H, Liu Z, Shi Z, Lu J, Suenaga K, et al. Mixed Low-Dimensional Nanomaterial: 2D Ultranarrow MoS₂ Inorganic Nanoribbons Encapsulated in quasi-1D Carbon Nanotubes. *J Am Chem Soc* (2010) 132:13840–7. doi: 10.1021/ja1058026
48. Wang L, Ye Y, Lu X, Wen Z, Li Z, Hou H, et al. Hierarchical Nanocomposites of Polyaniline Nanowire Arrays on Reduced Graphene Oxide Sheets for Supercapacitors. *Sci Rep* (2013) 3:5019–26. doi: 10.1038/srep03568

49. Li S, Liu Y, Zhao X, Shen Q, Zhao W, Tan Q, et al. Sandwich-Like Heterostructures of MoS₂/Graphene With Enlarged Interlayer Spacing and Enhanced Hydrophilicity as High-Performance Cathodes for Aqueous Zinc-Ion Batteries. *Adv Mater* (2021) 2007480:1–9. doi: 10.1002/adma.202007480
50. Wang C, Yu X, Park HS. Boosting Redox-Active Sites of 1T MoS₂ Phase by Phosphorus-Incorporated Hierarchical Graphene Architecture for Improved Li Storage Performances. *ACS Appl Mater Interfaces* (2020) 12:51329–36. doi: 10.1021/acsami.0c12414
51. Vaghiasya JV, Mayorga-Martinez CC, Sofer Z, Pumera M. Mxene-Based Flexible Supercapacitors: Influence of an Organic Ionic Conductor Electrolyte on the Performance. *ACS Appl Mater Interfaces* (2020) 12:53039–48. doi: 10.1021/acsami.0c12879
52. Shen J, Chen X, Wang P, Zhou F, Lu L, Wang R, et al. Electrochemical Performance of Zinc Carbodiimides Based Porous Nanocomposites as Supercapacitors. *Appl Surf Sci* (2021) 541:148355. doi: 10.1016/j.apsusc.2020.148355
53. Chen LX, Chen W, Jiang M, Lu Z, Gao C. Insights on the Dual Role of Two-Dimensional Materials as Catalysts and Supports for Energy and Environmental Catalysis. *J Mater Chem A* (2021) 9:2018–42. doi: 10.1039/d0ta08649e
54. Deng D, Novoselov KS, Fu Q, Zheng N, Tian Z, Bao X. Catalysis With Two-Dimensional Materials and Their Heterostructures. *Nat Nanotechnol* (2016) 11:218–30. doi: 10.1038/nnano.2015.340
55. Huang H, Wang Y, Zhang Y, Niu Z, Li X. Amino-Functionalized Graphene Oxide for Cr(VI), Cu(II), Pb(II) and Cd(II) Removal From Industrial Wastewater. *Open Chem* (2020) 18:97–107. doi: 10.1515/chem-2020-0009
56. Ahmad H, Huang Z, Kanagaraj P, Liu C. Separation and Preconcentration of Arsenite and Other Heavy Metal Ions Using Graphene Oxide Laminated With Protein Molecules. *J Hazard Mater* (2020) 384:121479. doi: 10.1016/j.jhazmat.2019.121479
57. Li DO, Gilliam MS, Debnath A, Chu XS, Yousaf A, Green AA, et al. Interaction of Pb²⁺ Ions in Water With Two-Dimensional Molybdenum Disulfide. *J Phys Mater* (2020) 3:024007. doi: 10.1088/2515-7639/ab7ab3
58. Oliveira NC, Maia MT, Noronha VT, Petry R, Aquino YMLO, Paula AJ. Nanomaterials for Desalination. *Elsevier Inc* (2019) 227–62. doi: 10.1016/B978-0-12-814829-7.00006-9
59. Liu G, Shen J, Liu Q, Liu G, Xiong J, Yang J, et al. Ultrathin Two-dimensional Mxene Membrane for Pervaporation Desalination. *J Memb Sci* (2017) 548:548–58. doi: 10.1016/j.memsci.2017.11.065
60. Safaei J, Xiong P, Wang G. Progress and Prospects of Two-Dimensional Materials for Membrane- Based Water Desalination. *Mater Today Adv* (2020) 8:100108. doi: 10.1016/j.mtadv.2020.100108
61. Heiranian M, Farimani AB, Aluru NR. Water Desalination With a Single-Layer MoS₂ Nanopore. *Nat Commun* (2015) 6(1):1–6. doi: 10.1038/ncomms9616
62. Caglar M, Silkina I, Brown BT, Thomeywork AL, Burton OJ, Babenko V, et al. Tunable Anion-Selective Transport Through Monolayer Graphene and Hexagonal Boron Nitride. *ACS Nano* (2020) 14:2729–38. doi: 10.1021/acsnano.9b08168
63. Ye S, Wang B, Pu Z, Liu T, Feng Y, Han W, et al. Flexible and Robust Porous Thermoplastic Polyurethane / Reduced Graphene Oxide Monolith With Special Wettability for Continuous Oil / Water Separation in Harsh Environment. *Sep Purif Technol* (2021) 266:118553. doi: 10.1016/j.seppur.2021.118553
64. Li Q, Zhang N, Yang Y, Wang G, Ng DHL. High Efficiency Photocatalysis for Pollutant Degradation With MoS₂/ C₃N₄ Heterostructures. *Langmuir* (2014) 30:8695–972. doi: 10.1021/la502033t
65. Online VA, Yang X, Li J, Liang T, Zhang Y, Chen H, et al. Antibacterial Activity of Two-Dimensional MoS₂ Sheets. *Nanoscale* (2014) 6:10126–33. doi: 10.1039/c4nr01965b
66. Guo X, Yue G, Huang J, Liu C, Zeng Q, Wang L. Label-Free Simultaneous Analysis of Fe (III) and Ascorbic Acid Using Fluorescence Switching of Ultrathin Graphitic Carbon Nitride Nanosheets. *ACS Appl Mater Interfaces* (2018) 10:26118–27. doi: 10.1021/acsami.8b10529
67. Huang H, Chen R, Ma J, Yan L, Zhao Y, Wang Y, et al. Graphitic Carbon Nitride Solid Nanofilms for Selective and Recyclable Sensing of Cu²⁺ and Ag⁺ in Water and Serum. *Chem Commun* (2014) 50:15415–8. doi: 10.1039/c4cc06659f
68. Ou JZ, Chrimes AF, Wang Y, Tang S, Strano MS, Kalantar-zadeh K. Ion-Driven Photoluminescence Modulation of Quasi-Two- Dimensional MoS₂ Nano Flakes for Applications in Biological Systems. *Nano Lett* (2014) 14:857–63. doi: 10.1021/nl4042356
69. Deng H, Yang X, Gao Z. MoS₂ Nanosheets as an Effective Fluorescence Quencher for DNA Methyltransferase Activity Detection. *Analyst* (2015) 140:3210–5. doi: 10.1039/c4an02133a
70. Wang L, Wang Y, Wong JI, Palacios T, Kong J, Yang HY. Functionalized MoS₂ nanosheet-based field-effect biosensor for label-free sensitive detection of cancer marker proteins in solution.. *Small* (2014) 10(6):1101–5. doi: 10.1002/sml.201302081
71. Lee KT, Liang YC, Lin HH, Li CH, Lu SY. Exfoliated SnS₂ Nanoplates for Enhancing Direct Electrochemical Glucose Sensing. *Electrochim Acta* (2016) 219:241–50. doi: 10.1016/j.electacta.2016.10.003
72. Singh C, Ali A, Kumar V, Ahmad R, Sumana G. Chemical Functionalized MoS₂ Nanosheets Assembled Microfluidic Immunosensor for Highly Sensitive Detection of Food Pathogen. *Sensors Actuators B Chem* (2018) 259:1090–8. doi: 10.1016/j.snb.2017.12.094
73. Elumalai S, Mani V, Jeromiyas N, Ponnusamy VK, Yoshimura M. A Composite Film Prepared From Titanium Carbide Ti₃C₂T_x (Mxene) and Gold Nanoparticles for Voltammetric Determination of Uric Acid and Folic Acid. *Microchim Acta* (2020) 187:1–10. doi: 10.1007/s00604-019-4018-0
74. Hernández-Sánchez D, Villabona-Leal G, Saucedo-Orozco I, Bracamonte V, Pérez E, Bittencourt C, et al. Stable Graphene Oxide-Gold Nanoparticle Platforms for Biosensing Applications. *Phys Chem Chem Phys* (2018) 20:1685–92. doi: 10.1039/c7cp04817c
75. Ji J, Wen J, Shen Y, Lv Y, Chen Y, Liu S, et al. Simultaneous Noncovalent Modification and Exfoliation of 2D Carbon Nitride for Enhanced Electrochemiluminescent Biosensing. *J Am Chem Soc* (2017) 139:11698–701. doi: 10.1021/jacs.7b06708
76. Lei Y, Butler D, Lucking MC, Zhang F, Xia T, Fujisawa K, et al. Single-Atom Doping of MoS₂ With Manganese Enables Ultrasensitive Detection of Dopamine: Experimental and Computational Approach. *Sci Adv* (2020) 6:1–9. doi: 10.1126/sciadv.abc4250
77. Fu Y, Zhang Y, Zheng S, Jin W. Bifunctional Electrochemical Detection of Organic Molecule and Heavy Metal At Two-Dimensional Sn-In₂S₃ Nanocomposite. *Microchem J* (2020) 159:105454. doi: 10.1016/j.microc.2020.105454
78. Peng Y, Zhou J, Song X, Pang K, Samy A, Hao Z, et al. A Flexible Pressure Sensor With Ink Printed Porous Graphene for Continuous Cardiovascular Status Monitoring. *Sensors (Switzerland)* (2021) 21:1–12. doi: 10.3390/s21020485
79. Ramalingam S, Elsayed A, Singh A. An Electrochemical Microfluidic Biochip for the Detection of Gliadin Using MoS₂/graphene/gold Nanocomposite. *Microchim Acta* (2020) 187(12):1–11. doi: 10.1007/s00604-020-04589-w
80. Moghzi F, Soleimannejad J, Sañudo EC, Janczak J. Dopamine Sensing Based on Ultrathin Fluorescent Metal-Organic Nanosheets. *ACS Appl Mater Interfaces* (2020) 12:44499–507. doi: 10.1021/acsami.0c13166
81. Noronha VT, Aquino YMLO, Maia MT, Freire RM. Sensing of Water Contaminants: From Traditional to Modern Strategies Based on Nanotechnology. *Elsevier Inc* (2019) 109–50. doi: 10.1016/B978-0-12-814829-7.00003-3
82. Kokulnathan T, Kumar EA, Wang TJ. Design and in Situ Synthesis of Titanium Carbide/Boron Nitride Nanocomposite: Investigation of Electrocatalytic Activity for the Sulfadiazine Sensor. *ACS Sustain Chem Eng* (2020) 8:12471–81. doi: 10.1021/acssuschemeng.0c03281
83. Purohit SD, Singh H, Bhaskar R, Yadav I, Bhushan S. Fabrication of Graphene Oxide and Nanohydroxyapatite Reinforced Gelatin – Alginate Nanocomposite Scaffold for Bone Tissue Regeneration. *Front Mater* (2020) 7:1–10. doi: 10.3389/fmats.2020.00250
84. Ramani D, Sastry TP. Bacterial Cellulose-Reinforced Hydroxyapatite Functionalized Graphene Oxide: A Potential Osteoinductive Composite. *Cellulose* (2014) 21:3585–95. doi: 10.1007/s10570-014-0313-4
85. Fu Y, Zhang JB, Lin H, Mo A. 2D Titanium Carbide(Mxene) Nanosheets and 1D Hydroxyapatite Nanowires Into Free Standing Nanocomposite

- Membrane: In Vitro and In Vivo Evaluations for Bone Regeneration. *Mater Sci Eng C* (2021) 118:111367. doi: 10.1016/j.msec.2020.111367
86. Liu X, George MN, Li L, Gamble D, Miller AL, Gaihe B, et al. Injectable Electrical Conductive and Phosphate Releasing Gel With Two-Dimensional Black Phosphorus and Carbon Nanotubes for Bone Tissue Engineering. *ACS Biomater Sci Eng* (2020) 6:4653–65. doi: 10.1021/acsbomaterials.0c00612
 87. Liu H, Yang G, Yin H, Wang Z, Chen C, Liu Z, et al. *In Vitro* and *In Vivo* Osteogenesis Up-Regulated by Two-Dimensional Nanosheets Through a Macrophage-Mediated Pathway. *Biomater Sci* (2021) 9:780–94. doi: 10.1039/d0bm01596b
 88. Le HuX, Kwon N, Yan KC, Sedgwick AC, Chen GR, He XP, et al. Bio-Conjugated Advanced Materials for Targeted Disease Theranostics. *Adv Funct Mater* (2020) 30:1–25. doi: 10.1002/adfm.201907906
 89. Ji X, Kong N, Wang J, Li W, Xiao Y, Gan ST, et al. A Novel Top-Down Synthesis of Ultrathin 2d Boron Nanosheets for Multimodal Imaging-Guided Cancer Therapy. *Adv Mater* (2018) 30:1803031. doi: 10.1002/adma.201803031
 90. Feng W, Wang R, Zhou Y, Ding L, Gao X, Zhou B, et al. Ultrathin Molybdenum Carbide MXene With Fast Biodegradability for Highly Efficient Theory-Oriented Photonic Tumor Hyperthermia. *Adv Funct Mater* (2019) 29:1–15. doi: 10.1002/adfm.201901942
 91. Lin H, Wang X, Yu L, Chen Y, Shi J. Two-Dimensional Ultrathin Mxene Ceramic Nanosheets for Photothermal Conversion. *Nano Lett* (2017) 17:384–91. doi: 10.1021/acs.nanolett.6b04339
 92. Murugan C, Sharma V, Murugan RK, Malaimegu G, Sundaramurthy A. Two-Dimensional Cancer Theranostic Nanomaterials: Synthesis, Surface Functionalization and Applications in Photothermal Therapy. *J Control Release* (2019) 299:1–20. doi: 10.1016/j.jconrel.2019.02.015
 93. Chen L, Chen C, Chen W, Li K, Chen X, Tang X, et al. Biodegradable Black Phosphorus Nanosheets Mediate Specific Delivery of hTERT siRNA for Synergistic Cancer Therapy. *ACS Appl Mater Interfaces* (2018) 10:21137–48. doi: 10.1021/acsami.8b04807
 94. Kang Y, Ji X, Li Z, Su Z, Zhang S. Boron-Based Nanosheets for Combined Cancer Photothermal and Photodynamic Therapy. *J Mater Chem B* (2020) 8:4609–19. doi: 10.1039/d0tb00070a
 95. Sekhon SS, Kaur P, Kim Y-H, Sekhon SS. 2D Graphene Oxide – Aptamer Conjugate Materials for Cancer Diagnosis. *Nat Partn Journals 2D Mater Appl* (2021) 5(1):1–19. doi: 10.1038/s41699-021-00202-7
 96. Zhan Y, Yan J, Wu M, Guo L, Lin Z, Qiu B, et al. Wong K Yin. Boron Nitride Nanosheets as a Platform for Fluorescence Sensing. *Talanta* (2017) 174:365–71. doi: 10.1016/j.talanta.2017.06.032
 97. Wang Q, Wang W, Lei J, Xu N, Gao F, Ju H. Fluorescence Quenching of Carbon Nitride Nanosheet Through its Interaction With DNA for Versatile Fluorescence Sensing. *Anal Chem* (2013) 85:12182–8. doi: 10.1021/ac403646n
 98. Qian X, Gu Z, Chen Y. Two-Dimensional Black Phosphorus Nanosheets for Theranostic Nanomedicine. *Mater Horizons* (2017) 4:800–16. doi: 10.1039/c7mh00305f
 99. Yang X, Wang D, Shi Y, Zou J, Zhao Q, Zhang Q, et al. Black Phosphorus Nanosheets Immobilizing Ce6 for Imaging-Guided Photothermal/Photodynamic Cancer Therapy. *ACS Appl Mater Interfaces* (2018) 10:12431–40. doi: 10.1021/acsami.8b00276
 100. Zhang N, Wang Y, Zhang C, Fan Y, Li D, Cao X, et al. Theranostics LDH-stabilized Ultrasmall Iron Oxide Nanoparticles as a Platform for Hyaluronidase-Promoted MR Imaging and Chemotherapy of Tumors. *Theranostics* (2020) 10(6):2791–802. doi: 10.7150/thno.42906
 101. Gonzalez-Rodriguez R, Campbell E, Naumov A. Multifunctional Graphene Oxide/Iron Oxide Nanoparticles for Magnetic Targeted Drug Delivery Dual Magnetic Resonance/ Fluorescence Imaging and Cancer Sensing. *PLoS One* (2019) 14:1–19. doi: 10.1371/journal.pone.0217072
 102. Guo Jj, Xia Ql, Wang Xg, Nie Yz, Xiong R, Guo Gh. Temperature and Thickness Dependent Magnetization Reversal in 2D Layered Ferromagnetic Material Fe₃GeTe₂. *J Magn Magn Mater* (2021) 527:167719. doi: 10.1016/j.jmmm.2020.167719
 103. Xu Z, Lu J, Zheng X, Chen B, Luo Y, Nauman M, et al. A Critical Review on the Applications and Potential Risks of Emerging MoS₂ Nanomaterials. *J Hazard Mater* (2020) 399:123057. doi: 10.1016/j.jhazmat.2020.123057
 104. Wang Z, Zhu W, Qiu Y, Yi X, Von Dem Bussche A, Kane A, et al. Biological and Environmental Interactions of Emerging Two-Dimensional Nanomaterials. *Chem Soc Rev* (2016) 45:1750–80. doi: 10.1039/c5cs00914f
 105. Zhou X, Sun H, Bai X. Two-Dimensional Transition Metal Dichalcogenides: Synthesis, Biomedical Applications and Biosafety Evaluation. *Front Bioeng Biotechnol* (2020) 8:236. doi: 10.3389/fbioe.2020.00236
 106. Yue H, Wei W, Yue Z, Wang B, Luo N, Gao Y, et al. The Role of the Lateral Dimension of Graphene Oxide in the Regulation of Cellular Responses. *Biomaterials* (2012) 33:4013–21. doi: 10.1016/j.biomaterials.2012.02.021
 107. Ma J, Liu R, Wang X, Liu Q, Chen Y, Valle RP, et al. Crucial Role of Lateral Size for Graphene Oxide in Activating Macrophages and Stimulating Pro-Inflammatory Responses in Cells and Animals. *ACS Nano* (2015) 9:10498–515. doi: 10.1021/acsnano.5b04751
 108. Orecchioni M, Jasim DA, Pescatori M, Manetti R, Fozza C, Sgarrella F, et al. Molecular and Genomic Impact of Large and Small Lateral Dimension Graphene Oxide Sheets on Human Immune Cells From Healthy Donors. *Adv Health Mater* (2016) 5:276–87. doi: 10.1002/adhm.201500606
 109. Cicuendez M, Fernandes M, Ayán-Varela M, Oliveira H, Feito MJ, Diez-Orejias R, et al. Macrophage Inflammatory and Metabolic Responses to Graphene-Based Nanomaterials Differing in Size and Functionalization. *Colloids Surf B Biointerfaces* (2020) 186:110709. doi: 10.1016/j.colsurfb.2019.110709
 110. Feito MJ, Diez-Orejias R, Cicuendez M, Casarrubios L, Rojo JM, Portolés MT. Characterization of M1 and M2 Polarization Phenotypes in Peritoneal Macrophages After Treatment With Graphene Oxide Nanosheets. *Colloids Surf B Biointerfaces* (2019) 176:96–105. doi: 10.1016/j.colsurfb.2018.12.063
 111. Feito MJ, Vila M, Matesanz MC, Linares J, Gonçalves G, Marques PAAP, et al. *In Vitro* Evaluation of Graphene Oxide Nanosheets on Immune Function. *J Colloid Interface Sci* (2014) 432:221–8. doi: 10.1016/j.jcis.2014.07.004
 112. Zhi X, Fang H, Bao C, Shen G, Zhang J, Wang K, et al. The Immunotoxicity of Graphene Oxides and the Effect of PVP-Coating. *Biomaterials* (2013) 34:5254–61. doi: 10.1016/j.biomaterials.2013.03.024
 113. Xu M, Zhu J, Wang F, Xiong Y, Wu Y, Wang Q, et al. Improved *In Vitro* and *In Vivo* Biocompatibility of Graphene Oxide Through Surface Modification: Poly(Acrylic Acid)-Functionalization is Superior to Pegylation. *ACS Nano* (2016) 10:3267–81. doi: 10.1021/acsnano.6b00539
 114. Gurunathan S, Kang M-H, Jeyaraj M, Kim J-H. Differential Immunomodulatory Effect of Graphene Oxide and Vanillin-Functionalized Graphene Oxide Nanoparticles in Human Acute Monocytic Leukemia Cell Line (Thp-1). *Int J Mol Sci* (2019) 20:247. doi: 10.3390/ijms20020247
 115. Yan J, Chen L, Huang C-C, Lung S-CC, Yang L, Wang W-C, et al. Consecutive Evaluation of Graphene Oxide and Reduced Graphene Oxide Nanoplatelets Immunotoxicity on Monocytes. *Colloids Surf B Biointerfaces* (2017) 153:300–9. doi: 10.1016/j.colsurfb.2017.02.036
 116. Zhou H, Zhao K, Li W, Yang N, Liu Y, Chen C, et al. The Interactions Between Pristine Graphene and Macrophages and the Production of Cytokines/Chemokines Via TLR- and NF- κ B-Related Signaling Pathways. *Biomaterials* (2012) 33:6933–42. doi: 10.1016/j.biomaterials.2012.06.064
 117. Li Y, Liu Y, Fu Y, Wei T, Le Guyader L, Gao G, et al. The Triggering of Apoptosis in Macrophages by Pristine Graphene Through the MAPK and TGF- β Signaling Pathways. *Biomaterials* (2012) 33:402–11. doi: 10.1016/j.biomaterials.2011.09.091
 118. Schinwald A, Murphy FA, Jones A, MacNee W, Donaldson K. Graphene-Based Nanoplatelets: A New Risk to the Respiratory System as a Consequence of Their Unusual Aerodynamic Properties. *ACS Nano* (2012) 6:736–46. doi: 10.1021/nn204229f
 119. Park E-J, Lee SJ, Lee K, Choi YC, Lee B-S, Lee G-H, et al. Pulmonary Persistence of Graphene Nanoplatelets may Disturb Physiological and Immunological Homeostasis. *J Appl Toxicol* (2017) 37:296–309. doi: 10.1002/jat.3361
 120. Cho YC, Pak PJ, Joo YH, Lee H-S, Chung N. *In Vitro* and *In Vivo* Comparison of the Immunotoxicity of Single- and Multi-Layered Graphene Oxides With or Without Pluronic F-127. *Sci Rep* (2016) 6:38884. doi: 10.1038/srep38884

121. Lin Y, Zhang Y, Li J, Kong H, Yan Q, Zhang J, et al. Blood Exposure to Graphene Oxide May Cause Anaphylactic Death in Non-Human Primates. *Nano Today* (2020) 35:100922. doi: 10.1016/j.nantod.2020.100922
122. de Luna LAV, Zorzi NE, de Moraes ACM, da Silva DS, Consonni SR, Giorgio S, et al. *In Vitro* Immunotoxicological Assessment of A Potent Microbicidal Nanocomposite Based on Graphene Oxide and Silver Nanoparticles. *Nanotoxicology* (2019) 13:189–203. doi: 10.1080/17435390.2018.1537410
123. Gong F, Chen M, Yang N, Dong Z, Tian L, Hao Y, et al. Bimetallic Oxide Few X Nanosheets as Multifunctional Cascade Bioreactors for Tumor Microenvironment-Modulation and Enhanced Multimodal Cancer Therapy. *Adv Funct Mater* (2020) 30:2002753. doi: 10.1002/adfm.202002753
124. Fang X, Wu X, Li Z, Jiang L, Lo W, Chen G, et al. Biomimetic Anti-PD-1 Peptide-Loaded 2d FePSe 3 Nanosheets for Efficient Photothermal and Enhanced Immune Therapy With Multimodal Mr/Pa/Thermal Imaging. *Adv Sci* (2021) 8:2003041. doi: 10.1002/advs.202003041
125. Liu X, Yan B, Li Y, Ma X, Jiao W, Shi K, et al. Graphene Oxide-Grafted Magnetic Nanorings Mediated Magnetothermodynamic Therapy Favoring Reactive Oxygen Species-Related Immune Response for Enhanced Antitumor Efficacy. *ACS Nano* (2020) 14:1936–50. doi: 10.1021/acsnano.9b08320
126. Han M, Zhu L, Mo J, Wei W, Yuan B, Zhao J, et al. Protein Corona and Immune Responses of Borophene: A Comparison of Nanosheet-Plasma Interface With Graphene and Phosphorene. *ACS Appl Bio Mater* (2020) 3:4220–9. doi: 10.1021/acsbm.0c00306
127. Wang X, Mansukhani ND, Guiney LM, Ji Z, Chang CH, Wang M, et al. Differences in the Toxicological Potential of 2D Versus Aggregated Molybdenum Disulfide in the Lung. *Small* (2015) 11:5079–87. doi: 10.1002/sml.201500906
128. Kurapati R, Muzi L, de Garibay APR, Russier J, Voiry D, Vacchi IA, et al. Enzymatic Biodegradability of Pristine and Functionalized Transition Metal Dichalcogenide MoS 2 Nanosheets. *Adv Funct Mater* (2017) 27:1605176. doi: 10.1002/adfm.201605176
129. Gu Z, Chen SH, Ding Z, Song W, Wei W, Liu S, et al. The Molecular Mechanism of Robust Macrophage Immune Responses Induced by PEGylated Molybdenum Disulfide. *Nanoscale* (2019) 11:22293–304. doi: 10.1039/C9NR04358F
130. Han Q, Wang X, Jia X, Cai S, Liang W, Qin Y, et al. Cpg Loaded MoS 2 Nanosheets as Multifunctional Agents for Photothermal Enhanced Cancer Immunotherapy. *Nanoscale* (2017) 9:5927–34. doi: 10.1039/C7NR01460K
131. Deng L, Pan X, Zhang Y, Sun S, Lv L, Gao L, et al. Immunostimulatory Potential of MoS2 Nanosheets: Enhancing Dendritic Cell Maturation, Migration and T Cell Elicitation. *Int J Nanomed* (2020) 15:2971–86. doi: 10.2147/IJN.S243537
132. Mo J, Xie Q, Wei W, Zhao J. Revealing the Immune Perturbation of Black Phosphorus Nanomaterials to Macrophages by Understanding the Protein Corona. *Nat Commun* (2018) 9:2480. doi: 10.1038/s41467-018-04873-7
133. Mo J, Xu Y, Wang X, Wei W, Zhao J. Exploiting the Protein Corona: Coating of Black Phosphorus Nanosheets Enables Macrophage Polarization Via Calcium Influx. *Nanoscale* (2020) 12:1742–8. doi: 10.1039/C9NR08570J
134. Raucci MG, Fasolino I, Caporali M, Serrano-Ruiz M, Soriente A, Peruzzini M, et al. Exfoliated Black Phosphorus Promotes *In Vitro* Bone Regeneration and Suppresses Osteosarcoma Progression Through Cancer-Related Inflammation Inhibition. *ACS Appl Mater Interfaces* (2019) 11:9333–42. doi: 10.1021/acsbm.9b021592
135. Su Y, Wang T, Su Y, Li M, Zhou J, Zhang W, et al. A Neutrophil Membrane-Functionalized Black Phosphorus Riding Inflammatory Signal for Positive Feedback and Multimodal Cancer Therapy. *Mater Horizons* (2020) 7:574–85. doi: 10.1039/C9MH01068H
136. Zhao H, Chen H, Guo Z, Zhang W, Yu H, Zhuang Z, et al. *In Situ* Photothermal Activation of Necroptosis Potentiates Black Phosphorus-Mediated Cancer Photo-Immunotherapy. *Chem Eng J* (2020) 394:124314. doi: 10.1016/j.cej.2020.124314
137. Song S-S, Xia B-Y, Chen J, Yang J, Shen X, Fan S-J, et al. Two Dimensional TiO 2 Nanosheets: *In Vivo* Toxicity Investigation. *RSC Adv* (2014) 4:42598–603. doi: 10.1039/C4RA005953K
138. Tang W, Dong Z, Zhang R, Yi X, Yang K, Jin M, et al. Multifunctional Two-Dimensional Core-Shell MXene@Gold Nanocomposites for Enhanced Photo-Radio Combined Therapy in the Second Biological Window. *ACS Nano* (2019) 13:284–94. doi: 10.1021/acsnano.8b05982
139. Xie Z, Chen S, Duo Y, Zhu Y, Fan T, Zou Q, et al. Biocompatible Two-Dimensional Titanium Nanosheets for Multimodal Imaging-Guided Cancer Theranostics. *ACS Appl Mater Interfaces* (2019) 11:22129–40. doi: 10.1021/acsbm.9b04628
140. Hao J, Song G, Liu T, Yi X, Yang K, Cheng L, et al. *In Vivo* Long-Term Biodistribution, Excretion, and Toxicology of PEGylated Transition-Metal Dichalcogenides Ms 2 (M = Mo, W, Ti) Nanosheets. *Adv Sci* (2017) 4:1600160. doi: 10.1002/advs.201600160
141. Qian X, Shen S, Liu T, Cheng L, Liu Z. Two-Dimensional TiS 2 Nanosheets for *In Vivo* Photoacoustic Imaging and Photothermal Cancer Therapy. *Nanoscale* (2015) 7:6380–7. doi: 10.1039/C5NR00893J
142. Lin H, Qiu W, Liu J, Yu L, Gao S, Yao H, et al. Silicene: Wet-Chemical Exfoliation Synthesis and Biodegradable Tumor Nanomedicine. *Adv Mater* (2019) 31:1903013. doi: 10.1002/adma.201903013
143. Xie H, Li Z, Sun Z, Shao J, Yu X-F, Guo Z, et al. Metabolizable Ultrathin Bi 2 Se 3 Nanosheets in Imaging-Guided Photothermal Therapy. *Small* (2016) 12:4136–45. doi: 10.1002/sml.201601050
144. Chen M, Chen S, He C, Mo S, Wang X, Liu G, et al. Safety Profile of Two-Dimensional Pd Nanosheets for Photothermal Therapy and Photoacoustic Imaging. *Nano Res* (2017) 10:1234–48. doi: 10.1007/s12274-016-1349-6
145. Orecchioni M, Ménard-Moyon C, Delogu LG, Bianco A. Graphene and the Immune System: Challenges and Potentiality. *Adv Drug Delivery Rev* (2016) 105:163–75. doi: 10.1016/j.addr.2016.05.014
146. Corbo C, Molinaro R, Parodi A, Toledano Furman NE, Salvatore F, Tasciotti E. The Impact of Nanoparticle Protein Corona on Cytotoxicity, Immunotoxicity and Target Drug Delivery. *Nanomedicine* (2016) 11:81–100. doi: 10.2217/nnm.15.188
147. Italiani P, Della Camera G, Boraschi D. Induction of Innate Immune Memory by Engineered Nanoparticles in Monocytes/Macrophages: From Hypothesis to Reality. *Front Immunol* (2020) 11:566309. doi: 10.3389/fimmu.2020.566309
148. Liu Z, He J, Zhu T, Hu C, Bo R, Wusiman A, et al. Lentinan-Functionalized Graphene Oxide Is an Effective Antigen Delivery System That Modulates Innate Immunity and Improves Adaptive Immunity. *ACS Appl Mater Interfaces* (2020) 12:39014–23. doi: 10.1021/acsbm.0c12078
149. Lebre F, Boland JB, Gouveia P, Gorman AL, Lundahl MLE, Lynch R, et al. Pristine Graphene Induces Innate Immune Training. *Nanoscale* (2020) 12:11192–200. doi: 10.1039/C9NR09661B
150. Su Y, Gao J, Kaur P, Wang Z. Neutrophils and Macrophages as Targets for Development of Nanotherapeutics in Inflammatory Diseases. *Pharmaceutics* (2020) 12:1222. doi: 10.3390/pharmaceutics12121222
151. Mukherjee SP, Gliga AR, Lazzaretto B, Brandner B, Fielden M, Vogt C, et al. Graphene Oxide is Degraded by Neutrophils and the Degradation Products are non-Genotoxic. *Nanoscale* (2018) 10:1180–8. doi: 10.1039/C7NR03552G
152. Moore C, Harvey A, Coleman JN, Byrne HJ, McIntyre J. *In Vitro* Localisation and Degradation of Few-Layer MoS 2 Submicrometric Plates in Human Macrophage-Like Cells: A Label Free Raman Micro-Spectroscopic Study. *2D Mater* (2020) 7:025003. doi: 10.1088/2053-1583/ab5d98
153. Grimaldi AM, Incoronato M, Salvatore M, Soricelli A. Nanoparticle-Based Strategies for Cancer Immunotherapy and Immunodiagnosics. *Nanomedicine* (2017) 12:2349–65. doi: 10.2217/nnm-2017-0208
154. De Pablo JJ, Jones B, Kovacs CL, Ozolins V, Ramirez AP. The Materials Genome Initiative, the Interplay of Experiment, Theory and Computation. *Curr Opin Solid State Mater Sci* (2014) 18:99–117. doi: 10.1016/j.cossms.2014.02.003
155. Schmidt J, Marques MRG, Botti S, Marques MAL. Recent Advances and Applications of Machine Learning in Solid-State Materials Science. *NPJ Comput Mater* (2019) 5:83. doi: 10.1038/s41524-019-0221-0
156. Schleder GR, Padilha ACM, Acosta CM, Costa M, Fazzio A. From DFT to Machine Learning: Recent Approaches to Materials Science—a Review. *J Phys Mater* (2019) 2:032001. doi: 10.1088/2515-7639/ab084b
157. Liu C, Chen H, Wang S, Liu Q, Jiang Y-G, Zhang DW, et al. Two-Dimensional Materials for Next-Generation Computing Technologies. *Nat Nanotechnol* (2020) 15:545–57. doi: 10.1038/s41565-020-0724-3

158. Tawfik SA, Isayev O, Stampfl C, Shapter J, Winkler DA, Ford MJ. Efficient Prediction of Structural and Electronic Properties of Hybrid 2d Materials Using Complementary DFT and Machine Learning Approaches. *Adv Theory Simul* (2019) 2:1800128. doi: 10.1002/adts.201800128
159. Giusti A, Atluri R, Tsekova R, Gajewicz A, Apostolova MD, Battistelli CL, et al. Nanomaterial Grouping: Existing Approaches and Future Recommendations. *NanoImpact* (2019) 16:100182. doi: 10.1016/j.impact.2019.100182
160. Basei G, Hristozov D, Lamon L, Zabeo A, Jeliazkova N, Tsiliki G, et al. Making Use of Available and Emerging Data to Predict the Hazards of Engineered Nanomaterials by Means of in Silico Tools: A Critical Review. *NanoImpact* (2019) 13:76–99. doi: 10.1016/j.impact.2019.01.003
161. Karcher S, Willighagen EL, Rumble J, Ehrhart F, Evelo CT, Fritts M, et al. Integration Among Databases and Data Sets to Support Productive Nanotechnology: Challenges and Recommendations. *NanoImpact* (2018) 9:85–101. doi: 10.1016/j.impact.2017.11.002
162. Lynch I, Afantitis A, Leonis G, Melagraki G, Valsami-Jones E. Strategy for Identification of Nanomaterials' Critical Properties Linked to Biological Impacts: Interlinking of Experimental and Computational Approaches. In *Advances in QSAR Modeling 2017*. (pp. 385–424). Springer, Cham.
163. Singh AV, Rosenkranz D, Ansari MHD, Singh R, Kanase A, Singh SP, et al. Artificial Intelligence and Machine Learning Empower Advanced Biomedical Material Design to Toxicity Prediction. *Adv Intell Syst* (2020) 2:2000084. doi: 10.1002/aisy.202000084
164. Afantitis A, Melagraki G, Isigonis P, Tsoumanis A, Varsou DD, Valsami-Jones E, et al. Nanosolveit Project: Driving Nanoinformatics Research to Develop Innovative and Integrated Tools for in Silico Nanosafety Assessment. *Comput Struct Biotechnol J* (2020) 18:583–602. doi: 10.1016/j.csbj.2020.02.023
165. Haase A, Klaessig F. EU Roadmap Nanoinformatics 2030. *EU Nanosafety Clust* (2018), 0–127. doi: 10.5281/zenodo.1486012
166. Cui Q, Hernandez R, Mason SE, Fraunheim T, Pedersen JA, Geiger F. Sustainable Nanotechnology: Opportunities and Challenges for Theoretical/Computational Studies. *J Phys Chem B* (2016) 120:7297–306. doi: 10.1021/acs.jpcc.6b03976
167. Winkler DA. Role of Artificial Intelligence and Machine Learning in Nanosafety. *Small* (2020) 16:2001883. doi: 10.1002/smll.202001883
168. Lynch I, Afantitis A, Exner T, Himly M, Lobaskin V, Doganis P, et al. Can An Inchi for Nano Address the Need for a Simplified Representation of Complex Nanomaterials Across Experimental and Nanoinformatics Studies? *Nanomaterials* (2020) 10:1–44. doi: 10.3390/nano10122493
169. Rajan K. Nanoinformatics: data-driven materials design for health and environmental needs. In *Nanotechnology Environmental Health and Safety 2014 Jan 1* (pp. 173–198). William Andrew Publishing.
170. Muratov EN, Bajorath J, Sheridan RP, Tetko IV, Filimonov D, Poroikov V, et al. QSAR Without Borders. *Chem Soc Rev* (2020) 49:3525–64. doi: 10.1039/d0cs00098a
171. Winkler DA. Recent Advances, and Unresolved Issues, in the Application of Computational Modelling to the Prediction of the Biological Effects of Nanomaterials. *Toxicol Appl Pharmacol* (2016) 299:96–100. doi: 10.1016/j.taap.2015.12.016
172. Trinh TX, Ha MK, Choi JS, Byun HG, Yoon TH. Curation of Datasets, Assessment of Their Quality and Completeness, and nanoSAR Classification Model Development for Metallic Nanoparticles. *Environ Sci Nano* (2018) 5:1902–10. doi: 10.1039/c8en00061a
173. Choi J-S, Ha MK, Trinh TX, Yoon TH, Byun H-G. Towards a Generalized Toxicity Prediction Model for Oxide Nanomaterials Using Integrated Data From Different Sources. *Sci Rep* (2018) 8:6110. doi: 10.1038/s41598-018-24483-z
174. Gajewicz A, Puzyn T, Odzimek K, Urbaszek P, Haase A, Riebeling C, et al. Decision Tree Models to Classify Nanomaterials According to the DF4nano Grouping Scheme. *Nanotoxicology* (2018) 12:1–17. doi: 10.1080/17435390.2017.1415388
175. Feng R, Yu F, Xu J, Hu X. Knowledge Gaps in Immune Response and Immunotherapy Involving Nanomaterials: Databases and Artificial Intelligence for Material Design. *Biomaterials* (2021) 266:120469. doi: 10.1016/j.biomaterials.2020.120469
176. Burello E. A Mechanistic Model for Predicting Lung Inflammogenicity of Oxide Nanoparticles. *Toxicol Sci* (2017) 159:339–53. doi: 10.1093/toxsci/kfx136
177. Ban Z, Yuan P, Yu F, Peng T, Zhou Q, Hu X. Machine Learning Predicts the Functional Composition of the Protein Corona and the Cellular Recognition of Nanoparticles. *Proc Natl Acad Sci U.S.A.* (2020) 117:10492–9. doi: 10.1073/pnas.1919755117
178. Quan X, Liu J, Zhou J. Multiscale Modeling and Simulations of Protein Adsorption: Progresses and Perspectives. *Curr Opin Colloid Interface Sci* (2019) 41:74–85. doi: 10.1016/j.cocis.2018.12.004
179. Duan Y, Coreas R, Liu Y, Bitounis D, Zhang Z, Parviz D, et al. Prediction of Protein Corona on Nanomaterials by Machine Learning Using Novel Descriptors. *NanoImpact* (2020) 17:100207. doi: 10.1016/j.impact.2020.100207
180. Alsharif SA, Power D, Rouse I, Lobaskin V. In Silico Prediction of Protein Adsorption Energy on Titanium Dioxide and Gold Nanoparticles. *Nanomaterials* (2020) 10:1–21. doi: 10.3390/nano10101967
181. Findlay MR, Freitas DN, Mobed-Miremadi M, Wheeler KE. Machine Learning Provides Predictive Analysis Into Silver Nanoparticle Protein Corona Formation From Physicochemical Properties. *Environ Sci Nano* (2018) 5:64–71. doi: 10.1039/C7EN00466D
182. Le TC, Yin H, Chen R, Chen Y, Zhao L, Casey PS, et al. An Experimental and Computational Approach to the Development of ZnO Nanoparticles That are Safe by Design. *Small* (2016) 12:3568–77. doi: 10.1002/smll.201600597
183. Mikolajczyk A, Gajewicz A, Mulkiewicz E, Rasulev B, Marchelek M, Diak M, et al. Nano-QSAR Modeling for Ecosafe Design of Heterogeneous TiO₂-Based Nano-Photocatalysts. *Environ Sci Nano* (2018) 5:1150–60. doi: 10.1039/C8EN00085A
184. Puzyn T, Rasulev B, Gajewicz A, Hu X, Dasari TP, Michalkova A, et al. Using nano-QSAR to Predict the Cytotoxicity of Metal Oxide Nanoparticles. *Nat Nanotechnol* (2011) 6:175–8. doi: 10.1038/nnano.2011.10
185. Wang W, Sedykh A, Sun H, Zhao L, Russo DP, Zhou H, et al. Predicting Nano-Bio Interactions by Integrating Nanoparticle Libraries and Quantitative Nanostructure Activity Relationship Modeling. *ACS Nano* (2017) 11:12641–9. doi: 10.1021/acsnano.7b07093
186. Martins C, Dreij K, Costa PM. The State-of-the Art of Environmental Toxicogenomics: Challenges and Perspectives of “Omics” Approaches Directed to Toxicant Mixtures. *Int J Environ Res Public Health* (2019) 16:1–16. doi: 10.3390/ijerph16234718
187. Peng T, Wei C, Yu F, Xu J, Zhou Q, Shi T, et al. Predicting Nanotoxicity by an Integrated Machine Learning and Metabolomics Approach. *Environ Pollut* (2020) 267:115434. doi: 10.1016/j.envpol.2020.115434
188. Serra A, Fratello M, Cattelani L, Liampa I, Melagraki G, Kohonen P, et al. Transcriptomics in Toxicogenomics, Part III: Data Modelling for Risk Assessment. *Nanomaterials* (2020) 10:708. doi: 10.3390/nano10040708
189. Ahmad F, Mahmood A, Muhmood T. Machine Learning-Integrated Omics for the Risk and Safety Assessment of Nanomaterials. *Biomater Sci* (2021) 9:1598–608. doi: 10.1039/D0BM01672A
190. Kinaret PAS, Ndika J, Ilves M, Wolff H, Vales G, Norppa H, et al. Toxicogenomic Profiling of 28 Nanomaterials in Mouse Airways. *Adv Sci* (2021) 2004588:2004588. doi: 10.1002/advs.202004588
191. Singh AV, Ansari MHD, Rosenkranz D, Maharjan RS, Kriegl FL, Gandhi K, et al. Artificial Intelligence and Machine Learning in Computational Nanotoxicology: Unlocking and Empowering Nanomedicine. *Adv Healthc Mater* (2020) 9:1901862. doi: 10.1002/adhm.201901862
192. Murugadoss S, Das N, Godderis L, Mast J, Hoet PH, Ghosh M. Identifying Nanodescriptors to Predict the Toxicity of Nanomaterials: A Case Study on Titanium Dioxide. *Environ Sci Nano* (2021) 8(2):580–90. doi: 10.1039/D0EN01031F
193. Papadiamantis AG, Jänes J, Voyiatzis E, Sikk L, Burk J, Burk P, et al. Predicting Cytotoxicity of Metal Oxide Nanoparticles Using Isalos Analytics Platform. *Nanomaterials* (2020) 10:1–19. doi: 10.3390/nano10102017
194. Milosevic A, Romeo D, Wick P. Understanding Nanomaterial Biotransformation: An Unmet Challenge to Achieving Predictive Nanotoxicology. *Small* (2020) 1907650. doi: 10.1002/smll.201907650
195. Papadiamantis AG, Klaessig FC, Exner TE, Hofer S, Hofstaetter N, Himly M, et al. Metadata Stewardship in Nanosafety Research: Community-Driven Organisation of Metadata Schemas to Support Fair Nanoscience Data. *Nanomaterials* (2020) 10:2033. doi: 10.3390/nano10102033
196. Martinez DST, Da Silva GH, de Medeiros AMZ, Khan LU, Papadiamantis AG, Lynch I. Effect of the Albumin Corona on the Toxicity of Combined Graphene Oxide and Cadmium to *Daphnia Magna* and Integration of the

- Datasets Into the NanoCommons Knowledge Base. *Nanomaterials* (2020) 10:1936. doi: 10.3390/nano10101936
197. Worth A, Aschberger K, Asturiol D, Bessems J, Gerloff K, Graepel R, et al. *Evaluation of the Availability and Applicability of Computational Approaches in the Safety Assessment of Nanomaterials*. Publications Office of the European Union, Luxembourg (2017). doi: 10.2760/248139
 198. Varsou DD, Afantitis A, Tsoumanis A, Melagraki G, Sarimveis H, Valsami-Jones E, et al. A Safe-by-Design Tool for Functionalised Nanomaterials Through the Enalos Nanoinformatics Cloud Platform. *Nanoscale Adv* (2019) 1:706–18. doi: 10.1039/c8na00142a
 199. Gazzi A, Fusco I, Orecchioni M, Ferrari S, Franzoni G, Yan JS, et al. Graphene, Other Carbon Nanomaterials and the Immune System: Toward Nanoimmunity-by-Design. *J Phys Mater* (2020) 3:034009. doi: 10.1088/2515-7639/ab9317
 200. Pinsino A, Bastús NG, Busquets-Fité M, Canesi L, Cesaroni P, Drobne D, et al. Probing the Immune Responses to Nanoparticles Across

Environmental Species. A Perspective of the EU Horizon 2020 Project PANDORA. *Environ Sci Nano* (2020) 7:3216–32. doi: 10.1039/D0EN00732C

Conflict of Interest: The authors declare that the research was conducted in the absence of any commercial or financial relationships that could be construed as a potential conflict of interest.

Copyright © 2021 Da Silva, Franqui, Petry, Maia, Fonseca, Fazzio, Alves and Martínez. This is an open-access article distributed under the terms of the Creative Commons Attribution License (CC BY). The use, distribution or reproduction in other forums is permitted, provided the original author(s) and the copyright owner(s) are credited and that the original publication in this journal is cited, in accordance with accepted academic practice. No use, distribution or reproduction is permitted which does not comply with these terms.